

Data-driven optimization of processes with degrading equipment

Johannes Wiebe¹, Inês Cecílio², and Ruth Misener¹

¹*Department of Computing, Imperial College London, London, UK*

²*Schlumberger Cambridge Research, Cambridge, UK*

Abstract

In chemical and manufacturing processes, unit failures due to equipment degradation can lead to process downtime and significant costs. In this context, finding an optimal maintenance strategy to ensure good unit health while avoiding excessive expensive maintenance activities is highly relevant. We propose a practical approach for the integrated optimization of production and maintenance capable of incorporating uncertain sensor data regarding equipment degradation. To this end, we integrate data-driven stochastic degradation models from Condition-based Maintenance into a process level mixed-integer optimization problem using Robust Optimization. We reduce computational expense by utilizing both analytical and data-based approximations and optimize the Robust Optimization parameters using Bayesian Optimization. We apply our framework to five instances of the State-Task-Network and demonstrate that it can efficiently compromise between equipment availability and cost of maintenance.

1 Introduction

Most technical processes contain equipment which degrades over time due to its usage. Degradation may lead to serious equipment failures, unless **preventive maintenance** actions are scheduled regularly to restore equipment conditions. While frequent preventive maintenance can keep equipment availability high, it also incurs significant cost. At the same time, unexpected equipment failures can lead to loss of production and high **corrective maintenance** costs. Finding the optimal balance between preventive and corrective maintenance is difficult, because degradation

tends to be at least partially random and the health state of equipment can often only be estimated from data subject to uncertainty. To make things worse, scheduling maintenance activities is not independent from production planning and scheduling. A unit undergoing maintenance might, for example, be unavailable for production. Furthermore, the state of equipment health tends to depend not only on the selected maintenance strategy, but also on the process operating strategy. Operating a process with a high throughput might enable higher production volumes and more sales, but could also cause more equipment degradation and therefore a higher maintenance cost. These interactions between process conditions, maintenance strategy, and the equipment's uncertain state of health make finding optimal and compatible maintenance and operating strategies a very challenging data-driven optimization problem under uncertainty.

One way of reducing the equipment maintenance cost is to determine maintenance schedules based on information regarding the equipment's state of health collected through condition monitoring¹. This is the **Condition-based maintenance** (CBM) paradigm¹⁻⁴. Due to the increased availability of cheap sensors and thereby large quantities of system health data, CBM is becoming more attractive⁵. While much attention has been paid to data collection & processing and prognostic modeling, the objective is usually to minimize the cost of maintaining a single unit⁴. This means that interaction between maintenance strategies for each piece of equipment and the operating strategy of the entire process has largely been neglected.

However, these interactions have been considered by multiple authors in the context of **integrated maintenance scheduling and process optimization**. Early approaches in this field which explicitly model degradation assume constant, known reliability or decay curves⁶⁻¹⁰. Dedopoulos and Shah^{6,7} combine short-term stochastic scheduling with long-term maintenance scheduling in a two-step procedure, while Vassiliadis and Pistikopoulos⁹ determine optimal availability thresholds at which maintenance should be performed. Georgiadis et al.¹¹ optimize the cleaning and energy management of heat exchanger networks subject to fouling, which is assumed to follow a known profile. Liu et al.¹² consider scheduling of maintenance and biopharmaceutical batch production with a deterministic performance decay. Xenos et al.¹³ optimize maintenance and production scheduling of a compressor network. The power consumed by the compressors is assumed to increase linearly with operating time (since maintenance was performed) due to fouling. Zulkafli and Kopanos^{14,15} develop an optimization framework for simultaneous operational planning and maintenance scheduling of production and utility systems. They consider extra energy costs caused by performance degradation. The degradation is assumed to depend on operating time and the production rate. Aguirre and Papageorgiou¹⁶ consider

integrated planning, scheduling and maintenance under schedule-dependent, deterministic performance decay. Rajagopalan et al.¹⁷ analyze turnaround rescheduling and apply stochastic programming to manage unplanned outages. Biondi et al.¹⁸ extend the State Task Network (STN), originally proposed by Kondili et al.¹⁹, to account for degrading equipment and different operating modes. They assume that each unit, after maintenance, has a given maximum residual lifetime and that each task performed on a unit in a certain operating mode reduces this residual lifetime by a given amount. Noticeably, none of these authors make use of the wealth of knowledge regarding degradation modeling and inference from data available from the CBM literature. Furthermore, degradation is assumed to be deterministic which may not be the case in practice.

Recent works have started to incorporate degradation models from CBM into process level Mixed-Integer Linear Programming (MILP) problems^{20–24}. Yildirim et al.^{20,21} formulate an optimization model for generator maintenance and production scheduling. The cost of maintenance is calculated beforehand using a data-driven degradation model:

$$c_t = \frac{c^{prev} (1 - p_t^f) + c^{corr} p_t^f}{\int_0^t p_\tau^f d\tau},$$

where c_t is the predicted cost of performing maintenance at time t given the cost of preventive (c^{prev}) and corrective (c^{corr}) maintenance. The failure probability $p_t^f = P(\text{unit fails before } t)$ is calculated from the degradation model. The authors later applied the same approach to maintenance and operation of wind farms and extended it to include opportunistic maintenance²². While this approach starts to incorporate information from more sophisticated degradation models into process level optimization problems, degradation is still considered to be deterministic in the MILP optimization. Başıftci et al.²³ extend this to consider sudden failures by using stochastic programming and generating scenarios from the underlying degradation model. To the best of our knowledge Başıftci et al.’s²³ approach is the only work combining stochastic optimization with information from degradation models.

Unfortunately, the aforementioned approach cannot capture effects of the selected operating strategy on degradation. Since maintenance cost is calculated based on the degradation model before the optimization problem is solved, the degradation is assumed to be independent of the operating strategy. In practice this will often not be the case.

This paper argues for a tighter integration between the sophisticated degradation models used in CBM and process level maintenance scheduling and process optimization. To this end we make multiple contributions:

- We show how Lévy type models, a class of stochastic processes commonly used in Degradation Modeling, can be incorporated into an integrated maintenance and process MILP model. Lévy type models include the Wiener and Gamma processes – two very popular models in CBM. By making the Lévy models parameters depend on a set of operating modes, equipment degradation too depends on the operating strategy.
- We show how uncertainty and randomness in the equipment’s degradation characteristics can be incorporated using adjustable robust optimization. We use results from the CBM literature to efficiently determine the robustness of the obtained solution.
- We prove that, in certain cases, feasible solutions to the adjustable robust optimization problem can be found by solving a deterministic approximation with worst case values for the uncertain parameters.
- Realizing that process planning and scheduling can be computationally expensive yet highly repetitive, we develop a computationally efficient, data-driven way of a-priori estimating equipment failure probabilities. To this end, we generate data using a short-term scheduling model repeatedly. Using this data, we propose two methods based on Logistic Regression capable of cheaply generating a large number of long-term schedules which can be used to estimate failure probabilities.
- We propose Bayesian optimization for efficiently optimizing the uncertainty set. The uncertainty set size depends on a small number of parameters, but solving the robust MILP integrated maintenance and process optimization problem can be computationally expensive. Bayesian optimization is ideal for this kind of low dimensional problem with expensive function evaluations.

As a challenging case study, we apply the proposed method to an extension of the state-task-network (STN)^{18,19}. This model combines both planning and scheduling of production and maintenance with operating mode dependent equipment degradation. We test our method on a number of STN instances^{19,25–28}.

2 Combining degradation modeling and robust optimization

Following Vassiliadis and Pistikopoulos⁹, we assume an integrated production and maintenance scheduling problem of the form

$$\min_{\mathbf{x}, \mathbf{m}} \quad \text{cost}(\mathbf{x}, \mathbf{m}) \quad (1)$$

$$\text{s.t.} \quad \text{process model}(\mathbf{x}, \mathbf{m}) \quad (1a)$$

$$\text{maintenance model}(\mathbf{x}, \mathbf{m}), \quad (1b)$$

where \mathbf{x} are the process variables (continuous and discrete) and \mathbf{m} are the maintenance related variables. The process model includes, e.g., material balances, energy balances, unit constraints, and the maintenance model includes, e.g., maintenance crew constraints or constraints regarding different types of maintenance. Note that cost minimization could easily be replaced by profit maximization.

A health model added to Problem 1 accounts for equipment degradation:

$$\min_{\mathbf{x}, \mathbf{m}, \mathbf{h}} \quad \text{cost}(\mathbf{x}, \mathbf{m}, \mathbf{h}) \quad (2)$$

$$\text{s.t.} \quad \text{process model}(\mathbf{x}, \mathbf{m}, \mathbf{h}) \quad (2a)$$

$$\text{maintenance model}(\mathbf{x}, \mathbf{m}, \mathbf{h}) \quad (2b)$$

$$\text{health model}(\mathbf{x}, \mathbf{m}, \mathbf{h}), \quad (2c)$$

where \mathbf{h} are health related variables and the health model includes all equipment health or degradation related constraints. Our first contribution is developing a generic health model based on the assumption that the equipments' state of health can be described by Lévy type processes, a class of stochastic processes commonly used for modeling degradation in CBM.

2.1 Degradation Modeling

The premise in Degradation Modeling is that a degradation signal $s^{meas}(t)$ describes the state of degradation of a unit over time. Signal $s^{meas}(t)$ can either be measured directly or obtained indirectly from measurements. Two common assumptions adopted in this paper are that:

(SMAX) The unit fails and requires corrective maintenance when $s^{meas}(t)$ crosses a threshold s^{max} ²⁹,

(AGAN) $s^{meas}(t)$ is reset back to initial value s^0 after preventive maintenance. The unit is as-good-as-new (AGAN)³⁰.

The degradation signal $s^{meas}(t)$ is often modeled by stochastic processes⁴. One class of stochastic processes are Lévy type processes:

Definition 1. Lévy type process³¹. A stochastic process $S(t) = \{S_t : t \in T\}$, where S_t is a random variable, with

1. independent increments: $S_{t_2} - S_{t_1}, \dots, S_{t_n} - S_{t_{n-1}}$ are independent for any $0 < t_1 < t_2 < \dots < t_n < \infty$,
2. stationary increments: $S_t - S_s$ and $S_{t-s} - S_0$ have the same distribution for any $s < t$,
3. continuity in probability: $\lim_{h \rightarrow 0} P(|S_{t+h} - S_t| > \epsilon) = 0$ for any $\epsilon > 0, t \geq 0$.

Lévy type processes include both the Wiener and Gamma processes, which are the most commonly used stochastic processes in the Degradation Modeling literature^{4,32-34}. Due to their independence and stationarity, Lévy type process increments can be described by

$$S_t - S_{t-\Delta t} = D(\Delta t), \quad D(\Delta t) \sim \mathcal{D}(\boldsymbol{\theta}, \Delta t), \quad \forall t, \quad (3)$$

where $D(\Delta t)$ is a random variable that follows a given distribution $\mathcal{D}(\boldsymbol{\theta}, \Delta t)$ with parameters $\boldsymbol{\theta}$. A difficulty, however, arises when \mathcal{D} is also dependent on some of the operational variables \boldsymbol{x} :

$$D(\Delta t) \sim \mathcal{D}(\boldsymbol{\theta}(\boldsymbol{x}), \Delta t). \quad (4)$$

This dependence has been addressed by assuming that the operational variables \boldsymbol{x} are piecewise constant, i.e., the process can only operate in a number of discrete operating modes $k \in K$ ^{35,36}. Under this assumption Eqns. 3 and 4 simplify to

$$S_t - S_{t-\Delta t} = \sum_{k \in \mathcal{K}} x_{k,t} \cdot D_k(\Delta t), \quad D_k(\Delta t) \sim \mathcal{D}(\boldsymbol{\theta}_k, \Delta t), \quad (5)$$

where $x_{k,t}$ is 1 if the process operates in mode k at time t and 0 otherwise. Note that this approach is very similar to regime-switching Lévy models used extensively in finance³⁷. Biondi et al.¹⁸ use a similar approach in their STN extension.

Much of the Degradation Modeling literature focuses on estimating $\boldsymbol{\theta}$ and using, e.g., Bayesian approaches to update it regularly based on new available data^{38,39}. A major advantage of Bayesian approaches is that $\boldsymbol{\theta}$ can be estimated based on a population of units first and then individually adjusted to a particular unit⁴⁰.

2.2 Constructing a health model

We summarize the assumptions on which health model 2c hereafter is based: For each process unit j , a degradation signal $s_j^{meas}(t)$ can be obtained from measurements which is modeled well by a Lévy process $S_j(t)$, i.e., increments follow Eqn. 5. The unit fails when $S_j(t)$ reaches a maximum threshold s_j^{max} (SMAx) ($T^{fail} = \inf\{t \in T | S_{j,t} > s_j^{max}\}$) and $S_j(t)$ resets to an initial value s_j^0 after maintenance (AGAN). Based on these assumptions and assuming a discrete time formulation, the following health model replaces Eqn. 2c:

$$S_{j,t} \leq s_j^{max} \quad \forall t, j \in J$$

$$S_{j,t} = \begin{cases} S_{j,t-1} + \sum_{k \in \mathcal{K}} x_{j,k,t} \cdot D_{j,k}, & \text{if } m_{j,t} = 0 \\ s_j^0, & \text{otherwise} \end{cases} \quad \forall t, j \in J, \quad (6)$$

where J is the set of process units and $m_{j,t}$ is 1 if a maintenance action starts on unit j at time t and 0 otherwise. To address the random nature of degradation, the random variables $D_{j,k}$ and $S_{j,t}$ can be approximated by an uncertain parameter $\tilde{d}_{j,k}$ and a deterministic variable $s_{j,t}$ respectively. Assuming that $\tilde{d}_{j,k}$ is bounded by a compact uncertainty set \mathcal{U} , Problem 2 can be robustified by requiring that all constraints hold for any $\tilde{d}_{j,k} \in \mathcal{U}$:

$$s_{j,t} \leq s_j^{max} \quad \forall t, j \in J$$

$$s_{j,t} = \begin{cases} s_{j,t-1} + \sum_{k \in \mathcal{K}} x_{j,k,t} \cdot \tilde{d}_{j,k}, & \text{if } m_{j,t} = 0 \\ s_j^0 & \text{otherwise} \end{cases} \quad \forall \tilde{d}_{j,k} \in \mathcal{U}, t, j \in J. \quad (7)$$

This model explicitly considers preventive maintenance. Corrective maintenance becomes necessary only when realizations of $\tilde{d}_{j,k}$ lie outside the uncertainty set \mathcal{U} and constraint $s_{j,t} \leq s_j^{max}$ is violated.

Notice that it is generally not possible to choose $s_{j,t}$ such that the equality constraint in Problem 7 holds for all values of $\tilde{d}_{j,k}$ in \mathcal{U} , except for the trivial solution $x_{j,k,t} = 0, \forall j, k, t$. This is because the degradation signal $s_{j,t}$ is an analytical variable, not a decision variable. Interpreting the degradation signal instead as a second stage variable $s_{j,t}(\tilde{d}_{j,k})$ turns Problem 7 into an adjustable robust optimization problem and a linear decision rule can be used to express $s_{j,t}$ as a function of $\tilde{d}_{j,k}$ ²⁵:

$$s_{j,t}(\tilde{d}_{j,k}) = [s_{j,t}]_0 + \sum_k [s_{j,t}]_k \tilde{d}_{j,k}, \quad (8)$$

where $[s_{j,t}]_0$ and $[s_{j,t}]_k$ are coefficients which become variables in the adjustable robust problem. Technically, $\tilde{d}_{j,k}$ should also be indexed by t as every time period constitutes

an independent realization of $D_{j,k}$. Time-indexed uncertain parameters have been previously explored²⁵, but they can lead to a large increase in variables, especially for discrete time formulations. We therefore make the simplifying assumption that uncertainty is only revealed once after all variables except $s_{j,t}$ have been selected.

The health model 7 can be reformulated to remove the conditional equality constraint, resulting in the final formulation:

$$\begin{aligned}
& \min_{\mathbf{x}, \mathbf{m}} \quad \text{cost}(\mathbf{x} = [x_{j,k,t}, \dots]^\top, \mathbf{m} = [m_{j,t}, \dots]^\top, \mathbf{h} = [s_{j,t} (\bar{d}_{j,k})]^\top) \\
& \text{s.t} \quad \text{process model}(\mathbf{x}, \mathbf{m}, \mathbf{h}) \\
& \quad \text{maintenance model}(\mathbf{x}, \mathbf{m}, \mathbf{h}) \\
& \quad m_{j,t} s_j^0 \leq s_{j,t} (\bar{d}_{j,k}) \leq s_j^{max} + m_{j,t} \cdot (s_j^0 - s_{j,max}) \quad \forall t, j \in J, \bar{d} \in \mathcal{U} \\
& \quad s_{j,t} (\bar{d}_{j,k}) \geq s_{j,t-\Delta t} + \sum_k x_{j,k,t} \tilde{d}_{j,k} + m_{j,t} \cdot (s_j^0 - s_j^{max}) \quad \forall t, j \in J, \bar{d} \in \mathcal{U} \\
& \quad s_{j,t} (\bar{d}_{j,k}) \leq s_{j,t-\Delta t} + \sum_k x_{j,k,t} \tilde{d}_{j,k} \quad \forall t, j \in J, \bar{d} \in \mathcal{U}.
\end{aligned} \tag{9}$$

By replacing $s_{j,t} (\bar{d}_{j,k})$ with Eqn. 8 in each constraint and using standard robust optimization reformulation techniques, the health model can be transformed into a deterministic robust counterpart (see Appendix A).

Consider a deterministic version of Problem 9 in which cost, process model, and maintenance model are not functions of $s_{j,t} (\bar{d}_{j,k})$ and $\bar{d}_{j,k}$ has been replaced by $d_{j,k}^{max} = \max_{\mathcal{U}} \tilde{d}_{j,k}$:

$$\begin{aligned}
& \min_{\mathbf{x}, \mathbf{m}} \quad \text{cost}(\mathbf{x}, \mathbf{m}) \\
& \text{s.t} \quad \text{process model}(\mathbf{x}, \mathbf{m}) \\
& \quad \text{maintenance model}(\mathbf{x}, \mathbf{m}) \\
& \quad m_{j,t} s_j^0 \leq s_{j,t}, \quad \forall t, j \in J \\
& \quad s_{j,t} \leq s_j^{max} + m_{j,t} (s_j^0 - s_j^{max}), \quad \forall t, j \in J \\
& \quad s_{j,t} \geq s_{j,t-1} + \sum_k x_{j,k,t} d_{j,k}^{max} + m_{j,t} (s_j^0 - s_j^{max}), \quad \forall t, j \in J \\
& \quad s_{j,t} \leq s_{j,t-1} + \sum_k x_{j,k,t} d_{j,k}^{max}, \quad \forall t, j \in J,
\end{aligned} \tag{10}$$

where $s_{j,t}$ is not a second stage variable anymore since there are no more semi-infinite constraints. Under certain circumstances, feasible solutions to robust Problem 9 can be found by solving deterministic Problem 10:

Theorem 1. *Given that cost, process model, and maintenance model are not functions of $\tilde{d}_{j,k}$ and that $s_j^0 \leq s_j^{init} = s_{j,t=t_0} \leq s_j^{max}$ and $\tilde{d}_{j,k} \geq 0, \forall \tilde{d}_{j,k} \in \mathcal{U}$, then a feasible solution ($\mathbf{x} = [x_{k,t}, \dots]$, $\mathbf{m} = [m_t, \dots]$, $\mathbf{h} = [s_t]$) to Problem 10 forms a feasible solution ($\mathbf{x} = [x_{k,t}, \dots]$, $\mathbf{m} = [m_t, \dots]$, $\mathbf{h} = [[s_t]_0, [s_t]_k]$) to Problem 9 with*

$$[s_t]_0 = \begin{cases} s^{init} & t < t_{m,0} \\ s^0 & t \geq t_{m,0} \end{cases} \quad (11a)$$

$$[s_t]_k = \sum_{t'=t_{m,t}}^t x_{k,t'}, \quad (11b)$$

where $s^{init} = s(t=0)$, $t_{m,0}$ is the first point in time at which maintenance is performed, and $t_{m,t}$ is the most recent point in time at which maintenance was performed.

Proof. See Appendix B □

Theorem 1 only guarantees solution feasibility, not optimality. How well Problem 10 approximates Problem 9 also depends on the selected uncertainty set.

2.3 The uncertainty set

A major decision in robust optimization is the uncertainty set choice. This paper uses a simple box uncertainty set

$$\mathcal{U} = \{\tilde{d}_{j,k} | \bar{d}_{j,k}(1 - \epsilon_{j,k}) \leq \tilde{d}_{j,k} \leq \bar{d}_{j,k}(1 + \epsilon_{j,k})\},$$

where $\bar{d}_{j,k}$ is the nominal value of $\tilde{d}_{j,k}$ and $\epsilon_{j,k}$ is a parameter determining the uncertainty set size. Note that this choice assumes that the random increments $D_{j,k}$ are independent, as a box uncertainty set cannot capture correlation between uncertain parameters. This assumption could be relaxed with a more complicated uncertainty set, e.g., a polyhedral set. Since Degradation Modeling assumes that the distribution of $D_{j,k}$ is known, $\epsilon_{j,k}$ can be determined using the inverse cumulative distribution function F^{-1} :

$$\epsilon_{j,k} = 1 - F^{-1}(\alpha)/\bar{d}_{j,k},$$

where $\alpha = P(D_{j,k} \leq \bar{d}_{j,k}(1 - \epsilon_{j,k}))$. If the distribution of $D_{j,k}$ is unknown, data-driven non-parametric methods such as Kernel Density Estimation can be used to estimate it⁴¹.

By using F^{-1} , the uncertainty set size depends on a single parameter $\alpha \in [0, 0.5]$. For $\alpha = 0$, the uncertainty set includes all possible realizations of $D_{j,k}$ and for $\alpha = 0.5$

the uncertainty set is a singleton and the robust optimization problem is equivalent to the deterministic problem using the nominal values $\bar{d}_{j,k}$. While box uncertainty sets are often more conservative than most of the many other available uncertainty set types^{42,43}, the solution robustness/conservatism in this formulation can be varied by adjusting α .

2.4 Evaluating robustness

Assume $\mathbf{x}_j^k = [k_1, k_2, \dots, k_T]$, where $k_t = k \iff x_{j,k,t} = 1$, is the sequence of operating modes given by a solution to Problem 9. Its robustness can be measured by the probability p_j that unit j does not fail in the time horizon T

$$p_j = P(S_{j,t} \leq S_{j,max}, \forall t < T | \mathbf{x}_j^k),$$

or equivalently its probability of failure

$$p_j^f = 1 - p_j = P(\exists t \text{ such that } S_{j,t} > S_{j,max} | \mathbf{x}_j^k).$$

Assuming the parameters $\boldsymbol{\theta}_{j,k}$ of the distributions $\mathcal{D}_{j,k}$ are estimated from data, p_j^f can be calculated through Monte-Carlo simulation by randomly generating N realizations $\mathbf{s}_j^n = [s_{j,0}^n, s_{j,\Delta t}^n, \dots, s_{j,T}^n]$ of $S_j(t, \mathbf{x}_j^k)$ with $\mathcal{D}_{j,k}(\boldsymbol{\theta}_{j,k}, \Delta t)$ distributed increments and checking how many violate $s_{j,t}^n \leq s_j^{max}$:

$$p_j^f = \frac{\sum_{n=1}^N \mathbb{1}(\exists t < T \text{ such that } s_{j,t}^n > s_j^{max})}{N}, \quad (12)$$

where $\mathbb{1}$ is the indicator function. This is illustrated in Fig. 1 for $N = 3$.

In the special case where $D_{j,k}$ is normal distributed $\mathcal{D}_{j,k} \sim \mathcal{N}(\mu_{j,k}\Delta t, \sigma_{j,k}^2\Delta t)$, i.e., the Wiener process model is used, p_j^f can be efficiently calculated using analytical results for the crossing probability of a Brownian motion on a piecewise linear boundary^{44,45}. Instead of sampling from $\mathcal{D}_{j,k}$ at regular time intervals Δt , this approach only randomly samples at operating mode transitions ($k_t \neq k_{t+1}$). It requires far less Monte-Carlo samples and is therefore faster than the general method outlined above. A detailed description of this approach is given in the Appendix D.

2.5 Estimating failure probabilities

Evaluating the probability of failure p_j^f , e.g., using Eqn. 12, requires the exact sequence of operating modes \mathbf{x}_j^k and maintenance actions to be known over the evaluation horizon T . Since maintenance tends to be infrequent, T has to be sufficiently

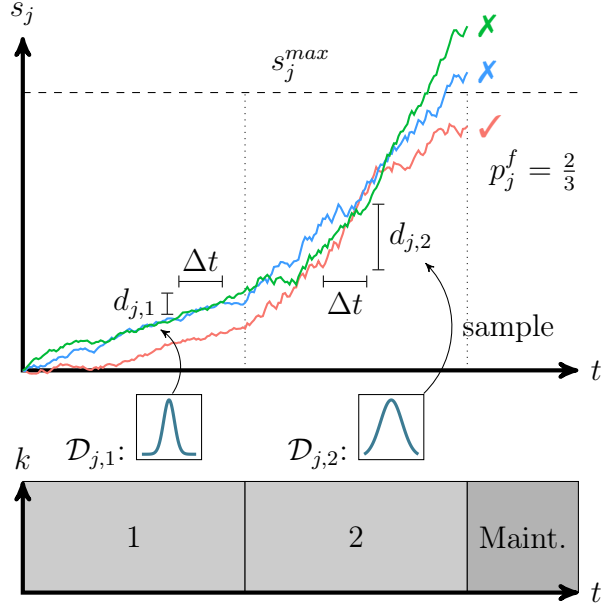


Figure 1: Example for calculating the failure probability p_j^f using Eqn. 12 and Monte-Carlo simulation. The operating mode schedule is $\mathbf{x}^k = [1, 2, \text{Maint.}]$.

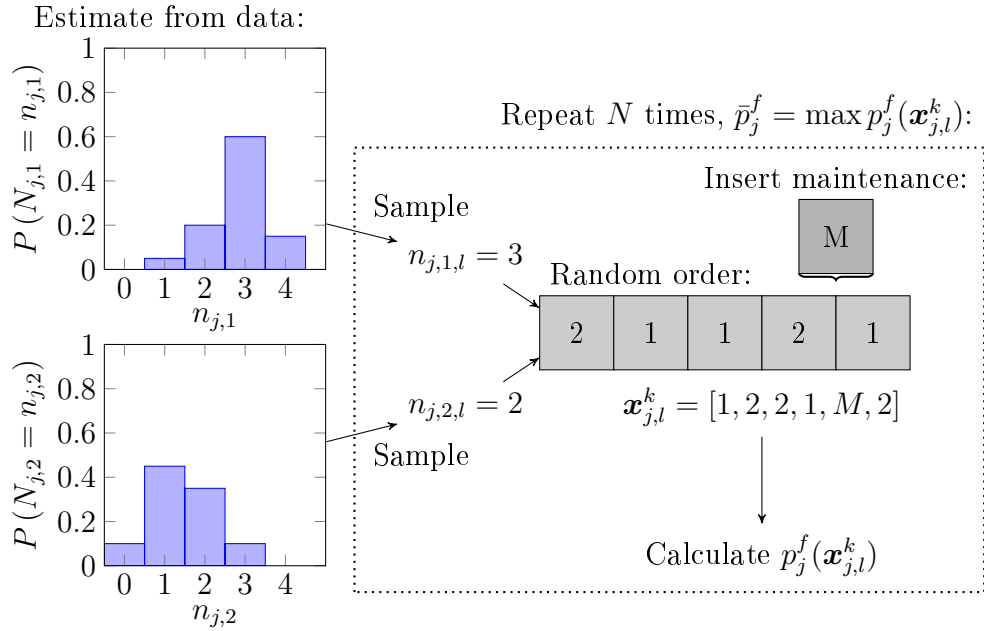


Figure 2: Frequency approach: Estimating p_j^f from historical data using Algorithm 1.

long to obtain meaningful failure probabilities. Solving Problem 9 over a long time horizon may be computationally challenging. Instead, it may be possible to use existing data of past schedules to estimate p_j^f . If no historical data is available, it can be generated by solving Problem 9 over a shorter horizon. This section outlines two methods by which an upper estimate of p_j^f can be obtained from data.

2.5.1 Frequency approach

Assuming time discretization, a conceptually easy way to obtain an upper bound \bar{p}_j^f on p_j^f is to generate the set \mathcal{X} of all possible permutations of operating mode sequences $\mathbf{x}_j^k = [k_{j,1}, k_{j,2}, \dots, k_{j,T}]$ and find the maximum probability of failure

$$\bar{p}_j^f = \max_{\mathbf{x} \in \mathcal{X}} p_j^f(\mathbf{x}_j^k).$$

For any realistic problem \mathcal{X} will be very large, but there are two ways to reduce its size: First, the operating mode sequences can be generated without considering maintenance. Maintenance actions can then be inserted consecutively at the latest point in time $t_{m,l}$ which satisfies

$$\max_{\tilde{d}_{j,k} \in \mathcal{U}} \sum_{t'=t_{m,l-1}}^{t_{m,l}} \sum_k x_{j,k,t'} \tilde{d}_{j,k} < s_j^{max} - s_j^0, \quad (13)$$

where $t_{m,l-1}$ is the previous maintenance activity and $t_{m,0} = 0$. \bar{p}_j^f remains an upper bound, because maintenance at a later point in time always causes a larger probability of failure. Secondly, it may be possible to estimate the frequency of occurrence $n_{j,k} = \sum_t x_{j,k,t}$ of each operating mode k from data. If these frequencies are modeled as random variables $N_{j,k}$, a smaller \mathcal{X} can be obtained by only generating sequences which obey frequencies drawn from the distributions of $N_{j,k}$. This suggests the following algorithm for obtaining an estimate of \bar{p}_j^f which is also visualized in Fig. 2:

If N is large enough and the estimated distribution of $N_{j,k}$ is accurate, \bar{p}_j^f should be a good upper bound on p_j^f .

2.5.2 Markov chain approach

The second approach for estimating \bar{p}_j^f is inspired by the use of Markov chains in regime-switching models in finance and to some extent also in the CBM literature for modeling different environmental or operating regimes of a process^{36,37,46,47}. The

Algorithm 1 Frequency approach [illustrated in Fig. 2]

```

1: procedure ESTIMATE  $\bar{p}_j^f$ 
2:    $\eta_{n_{j,k}} = P(N_{j,k} = n_{j,k}) \leftarrow$  estimate from historical data  $\forall n_k$ 
3:    $l \leftarrow 1$ 
4:   while  $l \leq N$  do
5:      $n_{j,k,l} \leftarrow$  draw random sample from  $P(N_{j,k} = n_{j,k})$  for each  $k$ 
6:      $\mathbf{x}_{j,l}^k \leftarrow$  arrange  $n_{j,l} = \sum_k n_{j,k,l}$  op. modes in random order  $[k_1, k_2, \dots, k_{n_{j,l}}]$ 
7:      $\mathbf{x}_{j,l}^k \leftarrow$  insert maintenance at last possible points in time  $\triangleright$  Eqn. 13
8:      $p_{j,l}^f \leftarrow p_j^f(\mathbf{x}_{j,l}^k)$   $\triangleright$  Eqn. 12
9:   end while
10:   $\bar{p}_j^f \leftarrow \max_{l \leq N} p_{j,l}^f$ 
11: end procedure

```

key idea is to treat the occurrence of operating modes k over time as a Markov chain. Modeling the sequence of operating modes \mathbf{x}_j^k on a unit by a memoryless Markov chain $X_j^k(t) = \{X_{j,t}^k : t \leq T\}$, the probability π_{k,k^*} of transitioning from one operating mode k to another k^* is given by

$$\pi_{k,k^*} = P(X_{j,t}^k = k^* | X_{j,t-1}^k = k).$$

The transition probabilities π_{k,k^*} can be estimated from data.

From this Markov chain random sequences of operating modes $\mathbf{x}_{j,l}^k$ can be generated. Maintenance can again be inserted at the latest possible point in time according to Eqn. 13. $\mathbf{x}_{j,l}^k$ may not be a feasible solution to Problem 9, but it can be used to estimate \bar{p}_j^f . The approach is summarized in Algorithm 2:

2.5.3 Logistic regression

The optimal sequence of operating modes $\mathbf{x}_j^{k,*}$ depends not only on the structure of the process and the size of the uncertainty set $\mathcal{U}(\alpha)$, but also on parameters $\boldsymbol{\psi}(t)$ such as product demands or environmental variables. The distributions of N_k and π_{k,k^*} are therefore not necessarily stationary:

$$\eta_{n_{j,k}}(\boldsymbol{\psi}(t)) = P(N_{j,k} = n_{j,k} | \boldsymbol{\psi}) \quad (14a)$$

$$\pi_{k,k^*}(\boldsymbol{\psi}(t)) = P(X_{j,t}^k = k^* | X_{j,t-1}^k = k, \boldsymbol{\psi}), \quad (14b)$$

where $\eta_{n_{j,k}}(\boldsymbol{\psi})$ is the probability that operating mode k occurs $n_{j,k}$ times in time period Δt .

Algorithm 2 Markov chain approach

- 1: **procedure** ESTIMATE \bar{p}_j^f
 - 2: $\pi_{k,k^*} = P(X_{j,t}^k = k^* | X_{j,t-1}^k = k) \leftarrow$ estimate from historical data $\forall(k, k^*)$
 - 3: $l \leftarrow 1$
 - 4: **while** $l \leq N$ **do**
 - 5: $\mathbf{x}_{j,l}^k \leftarrow$ draw random operating mode sequence from Markov chain π_{k,k^*}
 - 6: $\mathbf{x}_{j,l}^k \leftarrow$ insert maintenance at last possible points in time \triangleright Eqn. 13
 - 7: $p_{j,l}^f \leftarrow p_j^f(\mathbf{x}_{j,l}^k)$ \triangleright Eqn. 12
 - 8: **end while**
 - 9: $\bar{p}_j^f \leftarrow \max_{l \leq N} p_{j,l}^f$
 - 10: **end procedure**
-

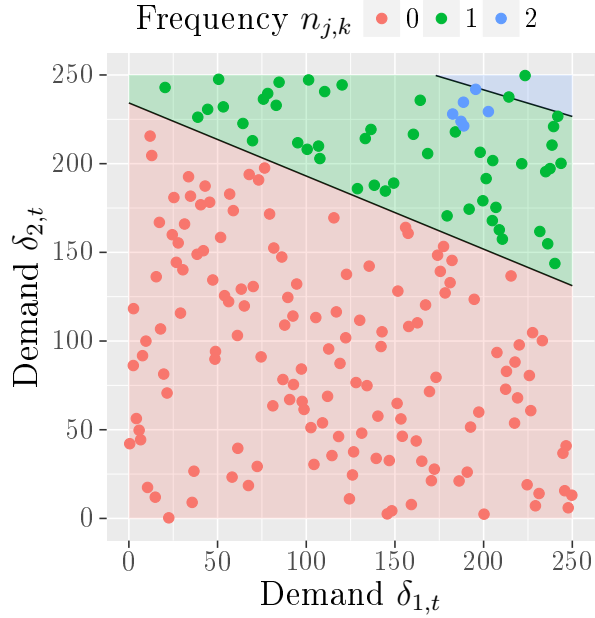


Figure 3: Frequency $n_{j,k}$ of operating mode k occurring on unit j for a scheduling problem with two product demands $\boldsymbol{\psi} = [\delta_{1,t}, \delta_{2,t}]^\top$. Points are training data generated by solving the scheduling model and shaded areas are predictions by logistic regression.

Covariate dependency of Markov chain transition probabilities has previously been modeled by using logistic regression^{48,49}. We model both $\eta_{n_{j,k}}$ and π_{k,k^*} using multinomial logistic regression in order to capture the influence of product demands:

$$\eta_{n_{j,k}}(\boldsymbol{\psi}(t)) = \frac{\exp(\boldsymbol{\beta}_{n_{j,k}}^\top \boldsymbol{\psi})}{\sum_{n'_k} \exp(\boldsymbol{\beta}_{n'_k}^\top \boldsymbol{\psi})} \quad (15a)$$

$$\pi_{k,k^*}(\boldsymbol{\psi}(t)) = \frac{\exp(\boldsymbol{\beta}_{k,k^*}^\top \boldsymbol{\psi})}{\sum_{k^+ \in K} \exp(\boldsymbol{\beta}_{k,k^+}^\top \boldsymbol{\psi})}. \quad (15b)$$

We use Scikit-learn⁵⁰ for estimating parameters $\boldsymbol{\beta}$ based on data. Fig. 3 shows an example for a process with two product demands $\boldsymbol{\psi} = [\delta_{1,t}, \delta_{2,t}]^\top$. The shaded areas are the frequencies $n_{j,k}$ predicted by logistic regression for a particular k and j (the $n_{j,k}$ with the largest $\eta_{n_{j,k}}(\boldsymbol{\psi})$) while the points are training data. We use logistic regression in this work because of its simplicity and interpretability, but it could be replaced by any classification method capable of probability estimation, e.g., Artificial Neural Networks, Support Vector Machines, k-Nearest Neighbours, Decision Trees, etc^{51,52}.

3 Optimizing the uncertainty set size

An important, non-trivial decision when using robust optimization is the size of the uncertainty set — or in this work the choice of parameter α . It governs a trade-off between the robustness of the solution and its cost. A common approach is to use a-priori guarantees to determine an uncertainty set size that is guaranteed to have a probability of constraint violation below a predefined level. A-priori guarantees are, however, not guaranteed to be tight and uncertainty sets based on them can be overly conservative. As demonstrated by Li and Li^{53,54}, determining the optimal uncertainty set size can instead be seen as its own optimization problem. They minimize the uncertainty set size with the constraint that the solution remains feasible with a pre-defined probability. We propose a different formulation that does not require the decision maker to choose a probability of constraint satisfaction but is based purely on cost instead:

$$\min_{\alpha} c^*(\alpha) + \sum_j p_j^f(\alpha) \cdot c_j^f, \quad (16)$$

where $c^*(\alpha)$ is the minimal overall cost of the process as determined by solving Problem 9 for a given value of α , p_j^f is the corresponding probability of failure

evaluated using Eqn. 12, and c_j^f is the cost incurred in case of an unplanned failure of unit j , i.e., the cost of corrective maintenance. Effectively, Problem 16 minimizes the trade-off between preventive and corrective maintenance. Note that this formulation assumes that each unit fails no more than once in the evaluated horizon T . This is reasonable under the assumption that the cost of failure c_j^f is high and therefore P_j^f tends to be low.

Problem 16 is a one-dimensional optimization problem, but determining $c^*(\alpha)$ and $p_j^f(\alpha)$ can be computationally expensive because it requires solving a potentially large MILP problem and Monte-Carlo simulation. It can therefore be viewed as a black box optimization problem with expensive function evaluations. We propose Bayesian optimization, which is known to work well on expensive low dimensional objective functions, as an effective solution strategy⁵⁵. Bayesian optimization has the further advantage that it can handle noise well. Both c^* and p_j^f can be noisy because it may not be possible to solve Problem 9 to optimality in a reasonable time frame. Further noise is introduced by the Monte-Carlo simulation used to evaluate p_j^f .

4 Case study

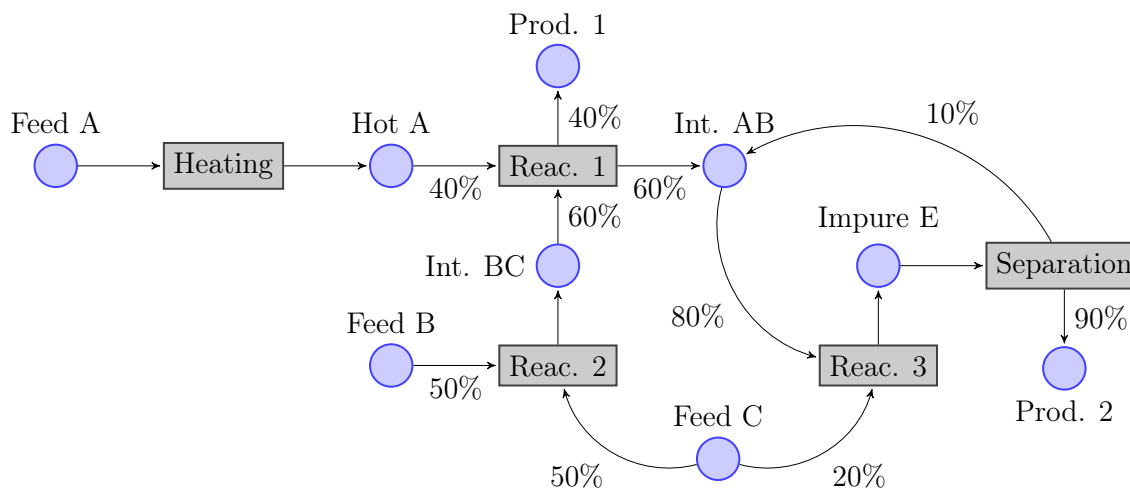


Figure 4: STN instance proposed by Kondili et al.¹⁹. Tasks are performed on four units: Heater, Reactor 1, Reactor 2, and Still.

The model by Biondi et al.¹⁸, an extension of the State-Task-Network (STN)¹⁹, forms the basis of our case study. The classic STN is a scheduling problem in which a set of tasks I has to be assigned to a set of units J . Biondi et al.¹⁸ extend the STN by allowing each task i to be performed in a number of different operating modes $k \in K_i$. They add constraints reducing the residual lifetime $r_{j,t}$ of each unit j every time a task is performed, and restore $r_{j,t}$ by performing maintenance. Because the scheduling problem can only be solved for a short time horizon T_S but maintenance occurs infrequently, they add a planning horizon T_P to the problem. For the planning horizon, instead of an exact schedule, only the number of times $n_{i,j,k,t}$ a task i is performed on unit j in operating mode k in each planning period t is calculated. Eqns. 17 to 20d give the modified version used as a case study in this work:

Objective function:

$$\begin{aligned} \text{cost} = & \sum_{j \in J} c_j^{maint} \left(s_j^{fin} / s_j^{max} + \sum_{t \in T} m_{j,t} \right) \\ & + c_s^{storage} \left(q_s^{fin} + \sum_{t \in T_p} q_{s,t} \right) \\ & + U \left(\sum_{s \in S} \phi_s^d + \sum_{t \in T_S} \phi_{s,t}^q \right) \end{aligned} \quad (17)$$

Constraints scheduling horizon:

$$\sum_{k \in K_j} \sum_{i \in I_j} \sum_{t' = t - p_{i,j,k} + \Delta t_S}^t w_{i,j,k,t'} + \sum_{t' = t - \tau_j + \Delta t_S}^t m_{j,t'} \leq 1 \quad \forall J, t \in T_S \quad (18a)$$

$$v_{i,j}^{min} w_{i,j,k,t} \leq b_{i,j,k,t} \leq v_{i,j}^{max} w_{i,j,k,t} \quad \forall J, i \in I_j, k \in K_j, t \in T_S \quad (18b)$$

$$\begin{aligned} q_{s,t} = & q_{s,t-1} + \sum_{i \in \bar{I}_s} \bar{\rho}_{i,s} \sum_{j \in J_i} \sum_{k \in K_j} b_{i,j,k,t-p_{i,j,k}} \\ & - \sum_{i \in I_s} \rho_{i,s} \sum_{j \in J_i} \sum_{k \in K_j} b_{i,j,k,t} \end{aligned} \quad \forall s, t \in T_S \quad (18c)$$

$$0 \leq q_{s,t} - \phi_{s,t}^q \leq c_s \quad \forall s, t \in T_S \quad (18d)$$

$$m_{j,t} s_j^0 \leq s_{j,t} \leq s_j^{max} + m_{j,t} \cdot (s_j^0 - s_j^{max}) \quad \forall t, j \in J, D \in \mathcal{U} \quad (18e)$$

$$s_{j,t} \geq s_{j,t-\Delta t_S} + \sum_i \sum_k w_{i,j,k,t} \tilde{d}_{j,k} + m_{j,t} \cdot (s_j^0 - s_j^{max}) \quad \forall t, j \in J, D \in \mathcal{U} \quad (18f)$$

$$s_{j,t} \leq s_{j,t-\Delta t_S} + \sum_i \sum_k w_{i,j,k,t} \tilde{d}_{j,k} \quad \forall t, j \in J, D \in \mathcal{U}, \quad (18g)$$

Constraints planning horizon:

$$\sum_{i \in I_j} \sum_{k \in K_j} p_{i,j,k} n_{i,j,k,t} + \tau_j m_{j,t} \leq \Delta t_P \quad \forall J, t \in T_P \setminus \{\bar{t}_P\} \quad (19a)$$

$$v_{i,j}^{\min} \sum_{k \in K_j} n_{i,j,k,t} \leq a_{i,j,t} \leq v_{i,j}^{\max} \sum_{k \in K_j} n_{i,j,k,t} \quad \forall J, i \in I_j, k \in K_j, t \in T_P \quad (19b)$$

$$q_{s,t} = q_{s,t-1} + \sum_{i \in \bar{I}_s} \bar{\rho}_{i,s} \sum_{j \in J_i} a_{i,j,t} - \sum_{i \in I_s} \rho_{i,s} \sum_{j \in J_i} a_{i,j,t} - \delta_{s,t} \quad \forall s, t \in T_P \setminus \{\bar{t}_P\} \quad (19c)$$

$$0 \leq q_{s,t} \leq c_s \quad \forall s, t \in T_P \quad (19d)$$

$$n_{i,j,k,t} \leq U \cdot \omega_{j,k,t} \quad \forall J, i \in I_j, k \in K_j, t \in T_P \quad (19e)$$

$$\sum_{k \in K_j} \omega_{j,k,t} = 1 \quad \forall J, t \in T_P \quad (19f)$$

$$s_{j,t} \leq s_j^{\max} \quad \forall t, j \in J \quad (19g)$$

$$s_j^t \geq s_{j,t-\Delta t_P} + \sum_k n_{j,k,t} \tilde{d}_{j,k,t} + m_{j,t} \cdot (s_j^0 - s_j^{\max}) \quad \forall t, j \in J \quad (19h)$$

$$s_{j,t} \leq s_{j,t-\Delta t_P} + \sum_k n_{j,k,t} \tilde{d}_{j,k,t} \quad \forall t, j \in J \quad (19i)$$

Constraints interface between scheduling and planning:

$$\begin{aligned} & \sum_{k \in K_j} \sum_{i \in I_j} \sum_{t'=\bar{t}_S+2\Delta t_S-p_{i,j,k}}^{\bar{t}_S} w_{i,j,k,t'} [p_{i,j,k} - (\bar{t}_S - t' + \Delta t_S)] \\ & + \sum_{t'=\bar{t}_S+2\Delta t_S-\tau_j}^{\bar{t}_S} m_{j,t'} [\tau_j - (\bar{t}_S - t' + \Delta t_S)] \quad \forall j \in J \quad (20a) \\ & + \sum_{i \in I_j} \sum_{k \in K_j} p_{i,j,k} n_{i,j,k,\bar{t}_P} + \tau_j m_{j,\bar{t}_P} \leq \Delta t_P, \end{aligned}$$

$$\begin{aligned} q_s^{\text{fin}} = q_{s,\bar{t}_S} + \sum_{i \in \bar{I}_s} \bar{\rho}_{i,s} \sum_{j \in J_i} \sum_{k \in K_j} b_{i,j,k,\bar{t}_S+1-p_{i,j,k}} \\ - \delta_{s,\bar{t}_S} + \phi_s^d \quad \forall s \quad (20b) \end{aligned}$$

$$0 \leq q_s^{fin} \leq c_s \quad \forall s \quad (20c)$$

$$q_{s,\bar{t}_P} = q_s^{fin} + \sum_{i \in \bar{I}_S} \bar{\rho}_{i,s} \sum_{j \in J_i} \sum_{k \in K_j} \sum_{t' = \bar{t}_s + 2 - p_{i,j,k}}^{\bar{t}_S} b_{i,j,k,t'} \\ + \sum_{i \in \bar{I}_S} \bar{\rho}_{i,s} \sum_{j, J_i} a_{i,j,\bar{t}_P} \quad \forall s \quad (20d) \\ - \sum_{i, I_s} \rho_{i,s} \sum_{j \in J_i} a_{i,j,\bar{t}_P} - \delta_{s,\bar{t}_P}$$

The decision variables are $m_{j,t}$, $q_{s,t}$, $w_{i,j,k,t}$, $n_{i,j,k,t}$, $b_{i,j,k,t}$, $a_{i,j,t}$, $s_{j,t}$, $\phi_{s,t}^q$, ϕ_s^d and $\omega_{j,k,t}$. The product demand $\delta_{s,t}$ has to be satisfied at the end of each planning period and at the end of any time interval in the scheduling horizon. In practice, this model would be solved regularly in a rolling horizon fashion using recent demand estimates and degradation signal measurements $s_{j,0}$.

In comparison to Biondi et al.¹⁸, the residual lifetime constraints have been replaced with the degradation signal based health model developed above (Eqn. 9). For the planning horizon, $s_{j,t}$ cannot be reset exactly to s_j^0 , because the exact time at which maintenance is performed is unknown. Instead, it is merely enforced that $s_{j,t} \leq s_j^{max}$.

In addition, the objective function is slightly different. The term $c_j^{maint}(s_j^{fin}/s_j^{max})$ can be interpreted as a final cost of maintenance dependent on the final degradation signal s_j^{fin} (state of health) of unit j . Similar to Biondi et al.'s¹⁸ penalty terms it avoids unnecessary degradation and ensures maintenance happens towards the end of a units residual lifetime.

Since the exact sequence of operating modes and maintenance actions is unknown in the planning horizon T_P , the probability of failure p_j^f can only be evaluated over the scheduling horizon T_S . In order to still evaluate p_j^f over a longer time period two possibilities exist: the schedule can be extended in length by solving the model repeatedly in a rolling horizon fashion or the Markov chain-based estimation approach in Algorithm 2 can be used. We compare both approaches to show that the proposed Markov chain estimate is indeed accurate. Note that, in order to facilitate a rolling horizon based solution approach, slack variables have been introduced in Eqns. 18d and 20b. This is necessary because the rolling horizon framework does not guarantee feasibility in subsequent time periods. Production targets from the planning model may, for example, not be achievable in the scheduling model. The slack variables ϕ_s^d and $\phi_{s,t}^q$ are penalized in the objective function.

We assume that the frequencies of operating mode occurrence $n_{j,k}$ and the transition probabilities π_{k,k^*} depend on the product demands in each planning period

($\phi_t = [d_{s_1,t}, \dots, d_{s_n,t}]$). We sample a range of demands using Latin Hypercube Sampling and solve just the scheduling horizon to generate data for estimating $n_{j,k}(\psi_t)$ and $\pi_{k,k^*}(\psi_t)$.

Notice that the model above fulfills the assumptions in Theorem 1 and solutions can be obtained by solving the deterministic approximation 10.

5 Results

The framework outlined above was evaluated on five instances of the STN (see Table 1 and Appendix C). The model was implemented in Pyomo^{56,57} and solved using

Instance	Toy	P1 ¹⁹	P2 ²⁶	P4 ²⁷	P6 ²⁸
Units	2	4	5	3	6
Tasks	3	5	3	4	8
Op. modes	2	3	3	2	2
Products	2	2	1	2	4
Discrete vars	518	2492	1930	1869	1993
Continuous vars	1033	3630	2371	2777	4084
Constraints	1860	7332	5705	5699	7994
Avg. MIP gap [%]	0.0	3.0	5.8	10.9	1.02

Table 1: Evaluated STN instances (Details: see Appendix C)

CPLEX 12.7.1.0. All source code is publicly available under the MIT Licence⁵⁸. Unless mentioned otherwise, we considered an evaluation horizon of 12 planning periods. The failure probability p_j^f for each unit j was evaluated for a range of values of the uncertainty set parameter α using both the frequency and Markov chain estimates as well as rolling horizon. The termination criteria for each CPLEX run were a maximum time limit between 1 – 5 minutes (depending on the size of the instance) and a MIP gap of 2% (except for the toy instance which was solved to optimality). For each instance a low, average, and high demand scenario was considered with the high scenario being close to maximum process capacity. For Instance P1¹⁹ both the robust and deterministic Problems 9 and 10 were solved a number of times to evaluate the quality of the deterministic approximation. For all other instances only the deterministic approach was used. All calculations were carried on an i7-6700 CPU with 8×3.4 GHz and 16GB RAM.

Fig. 5 shows three maintenance schedules for the original STN instance (P1) by Kondili et al.¹⁹ with Biondi et al.’s¹⁸ demand scenario (average scenario) with

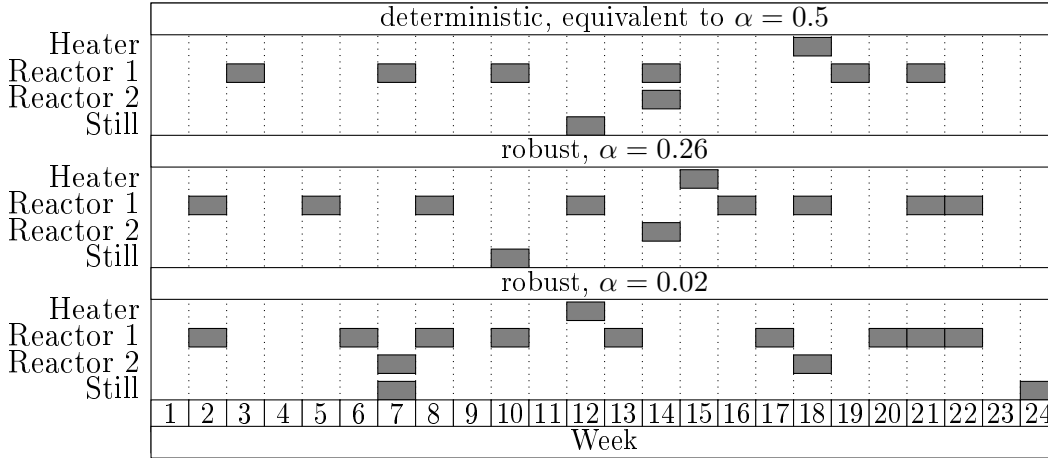


Figure 5: Comparison of maintenance schedules between deterministic solution ($\alpha = 0.5$) and two robust solutions with different values of α (Instance P1¹⁹, average demand scenario by Biondi et al.¹⁸). The number of required maintenance actions increases with increasing uncertainty set size (decreasing α).

different values for α . The number of maintenance actions increases with increasing uncertainty set size (decreasing α). Essentially, hedging against more uncertainty and ensuring solution robustness for a larger set of possible realizations requires earlier maintenance. In the average demand scenario, maintenance actions increase by 22% when hedging against some of the uncertainty ($\alpha = 0.26$) and by 56% when hedging against almost all uncertainty ($\alpha = 0.02$). However, this trend also depends on product demand: for the low demand scenario, only an increase of 25% is necessary for $\alpha = 0.02$, while an increase of 64% is necessary in the high demand scenario. A higher demand increases unit utilization and therefore also the absolute number of maintenance actions required in a given time period.

Fig. 6 shows the failure probability p_j^f for Reactor 1 as a function of both total cost (cost of storage and cost of maintenance) and the uncertainty set parameter α . As expected, p_j^f increases for smaller uncertainty sets (large α 's) and a low p_j^f comes at a significant cost – the price of robustness. Notice that, while calculating p_j^f using Monte-Carlo simulation only introduces modest noise, the calculated cost is very noisy due to the non-optimality of the solutions.

The results in Fig. 6 were obtained by solving the deterministic Problem 10. While Theorem 1 guarantees that these solutions are also feasible in the robust Problem 9, it does not prove that they are also optimal. Fig. 7 shows both total cost

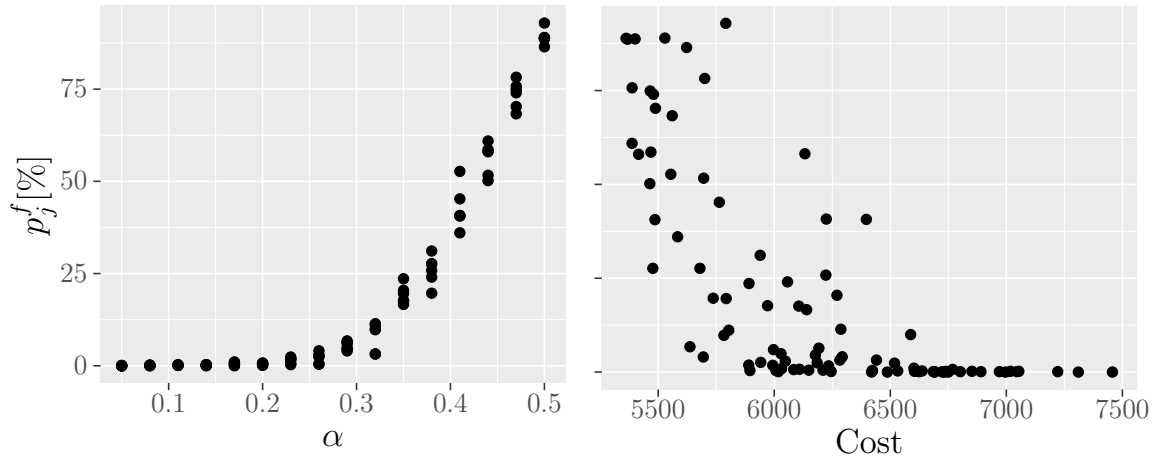


Figure 6: Probability of Reactor 1 failing p_j^f vs uncertainty set parameter α and cost (Instance P1¹⁹, average demand scenario). Each point is a solution to Problem 10 obtained by CPLEX. The probability of failure p_j^f was estimated using the Algorithm 2 Markov chain approach.

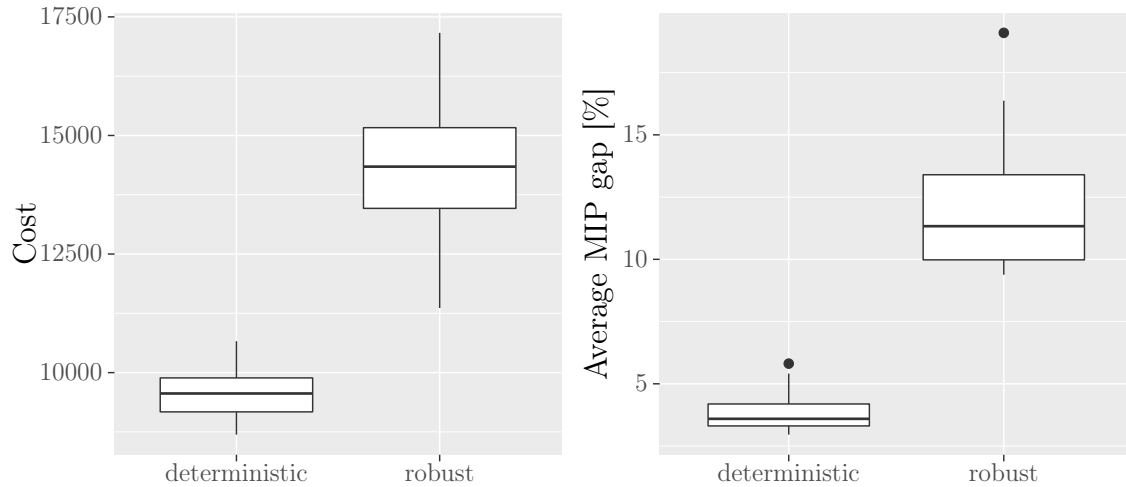


Figure 7: Robust vs. deterministic approach (Instance P1¹⁹). Each model was solved 25 times with $\alpha = 0.41$ and a 120s time limit per rolling horizon iteration using out-of-the-box CPLEX. The robust model has 22514 variables and 14664 constraints while the deterministic model has 6122 variables and 7332 constraints.

and average optimality gap for a number of rolling horizon solutions to the deterministic and robust version of Instance P1¹⁹. The uncertainty set size was $\alpha = 0.41$ and a maximum time limit of 120s was used for each CPLEX run. Within this time limit, out-of-the-box CPLEX achieves an average optimality gap of 12.1% on the robust problem compared with 3.8% for the deterministic approximation with maximum values for $\tilde{d}_{j,k}$. Similarly, the deterministic approximation achieves significantly lower objective values. While many approaches could improve solution quality of the robust problem, e.g., solver parameter tuning or leveraging Satisfiability Modulo Theory⁵⁹, Constraint Programming⁶⁰, or Approximation Algorithms⁶¹, it is likely that the deterministic approximation will remain favorable as it has significantly fewer variables and constraints (6122 vs. 22514 and 7332 vs. 14664 respectively). Assuming a box uncertainty set, we view it as a reasonable approximation for instances which cannot be solved to optimality in a reasonable amount of time. In the case of a more complex uncertainty set, replacing $\tilde{d}_{j,k}$ with its maximum value may lead to conservative solutions. General uncertainty sets require solving the robust problem.

Note that the large range of solution values in Fig. 7 is not only due to the differing MIP gaps, but also the rolling horizon approach which does not guarantee optimality.

Logistic regressions for the Frequency and Monte-Carlo approaches were trained based on 200 scheduling horizon only solutions. For the Frequency approach, the training points and their predicted values for Reaction 1 in mode Normal of the toy instance are shown in Fig. 8. Logistic regression predicts $n_{i,j,k}$ reasonably well but the rigid, linear classifier cannot capture some of the details. This is, however, not a major problem as the entire predicted probability distribution $\eta_{n_{i,j,k}}$ of operating mode occurrence frequencies $n_{i,j,k}$ is used in estimating \bar{p}_j^f . Near the predicted boundaries, $\eta_{n_{i,j,k}}$ of adjacent frequencies will be non-zero and they will be sampled in a significant number of operating mode sequences in Algorithm 1.

Fig. 9 shows the probability of failure p_j^f for each unit in the toy instance as a function of the uncertainty set parameter α for three different demand scenarios (average, high, and low). Since the rolling horizon framework does not guarantee optimality, solving the problem repeatedly for the same value of α can lead to different solutions and failure probabilities. The problem was therefore solved 10 times for each value of α . It can be seen that the probability of failure generally increases with demand. The figure furthermore shows the two bounds obtained using the Frequency and Markov chain based approaches, i.e. Algorithm 1 versus 2. For the reactor both approaches provide good upper bounds. For the heater, the frequency based approach performs very well, while the Markov chain approach underestimates p_j^f for the high demand scenario and overestimates it for the average and low demand

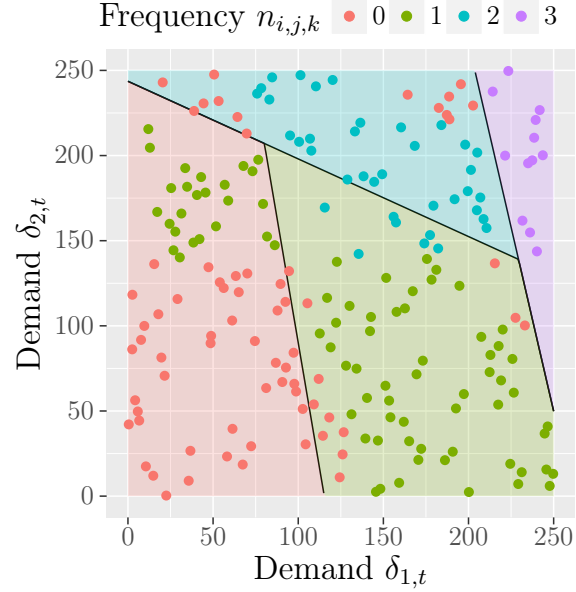


Figure 8: Toy instance: Frequency $n_{i,j,k}$ of Reaction 1 occurring in normal mode on unit Reactor within one scheduling horizon. Points are training data generated by solving the scheduling model repeatedly and shaded areas are predictions by logistic regression.

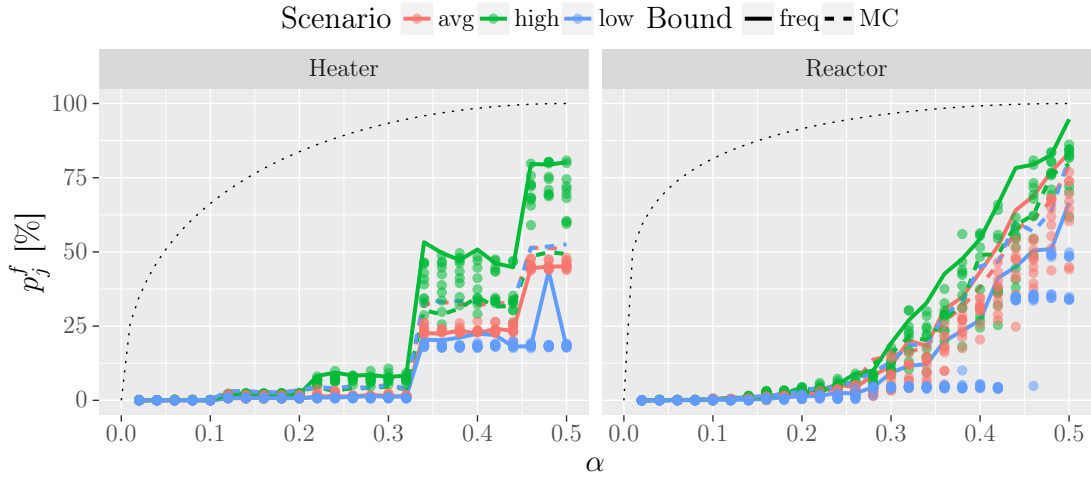


Figure 9: Toy instance: Frequency vs. Markov chain approach. Points are rolling horizon solutions. Colored lines are bounds from the Frequency and Markov chain approach. The dotted black lines show a-priori bound B4 by Li et al. ⁶².

scenarios. Finally notice that the apriori bound⁶² given by the dotted lines greatly overestimates p_j^f . Fig. 10 shows similar trends for Instance P1¹⁹ (Kondili). Both approaches provide reasonable bounds for all units and scenarios except the average demand scenario on the Heater, for which the frequency approach underestimates p_j^f . Notice that p_j^f is nearly zero for both the Heater and Reactor 2 at low demand irrespective of α . This is because for this scenario no maintenance occurs on either unit and $s_{j,t}$ does not get close to s_j^{max} .

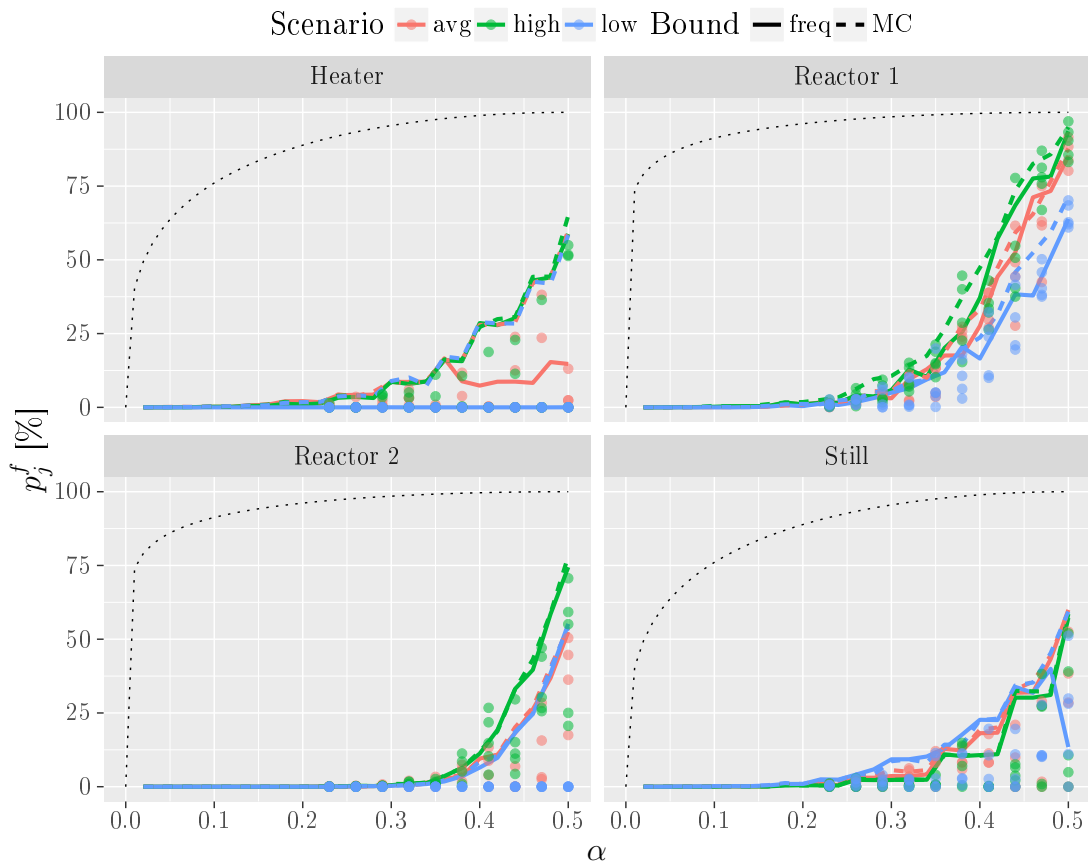


Figure 10: Instance P1¹⁹: Frequency vs. Markov chain approach. Points are rolling horizon solutions. Colored lines are bounds from the Frequency and Markov chain approach. The dotted black lines show a-priori bound B4 by Li et al.⁶².

The performance of the Frequency and Markov chain based probability estimates

was assessed using three metrics:

$$\text{rms}_{all}^2 = \frac{1}{N \cdot |A|} \sum_{n \in \{1..N\}, \alpha \in A} \left(\left[p_j^f \right]_{n,\alpha} - \bar{p}_j^f \right)^2, \quad (21a)$$

$$p_{out} = \frac{1}{N \cdot |A|} \sum_{n \in \{1..N\}, \alpha \in A} \mathbb{1} \left(\left[p_j^f \right]_{n,\alpha} > \bar{p}_j^f \right), \text{ and} \quad (21b)$$

$$\text{rms}_{out}^2 = \frac{1}{p_{out} \cdot N \cdot |A|} \sum_{n \in \{1..N\}, \alpha \in A} \mathbb{1} \left(\left[p_j^f \right]_{n,\alpha} > \bar{p}_j^f \right) \left(\left[p_j^f \right]_{n,\alpha} - \bar{p}_j^f \right)^2, \quad (21c)$$

where rms_{all} is the root-mean-squared deviation between the estimate and all rolling horizon solutions, p_{out} is the percentage of rolling horizon solutions with a larger p_j^f than the estimated bound, and rms_{out} is the root-mean-squared deviation of all underestimated points. While rms_{all} evaluates the estimate \bar{p}_j^f 's quality as a predictor of p_j^f , p_{out} and rms_{out} assess its quality as an upper bound.

instance	bound	rms_{all}	p_{out}	rms_{out}
toy	freq	8.00	17.54	0.90
toy	mc	10.41	9.62	2.86
P1 ¹⁹	freq	12.61	18.08	5.80
P1	mc	17.25	10.13	1.81
P2 ²⁶	freq	7.40	48.19	2.24
P2	mc	13.68	40.56	1.10
P4 ²⁷	freq	10.09	13.77	4.10
P4	mc	11.40	11.91	2.67
P6 ²⁸	freq	16.35	29.40	4.48
P6	mc	20.16	21.27	3.23
all	freq	10.89	25.40	3.50
all	mc	14.58	18.70	2.34

Table 2: Average performance metrics for probability estimates - all instances

Table 2 shows values for all three instances averaged over demand scenarios and units for all tested STN instances. It can be seen that the frequency approach is generally a better estimator for p_j^f than the Markov chain approach (smaller values of rms_{all}) but also has a larger rate of misclassification p_{out} . While rms_{all} can be large due to noise in the rolling horizon solutions and p_{out} values of up to 48% show that \bar{p}_j^f is not a perfect upper bound, rms_{out} is generally small with average values

of 3.50 and 2.34% for the Frequency and Markov chain approach respectively. This means that, when \bar{p}_j^f underestimates p_j^f , it does not do so by much. Considering the noise introduced by non-optimal solutions and the rolling horizon framework, the error introduced by estimating p_j^f through \bar{p}_j^f is small. Because it is a slightly better upper bound, the Markov chain approach was used for all subsequent experiments unless mentioned otherwise.

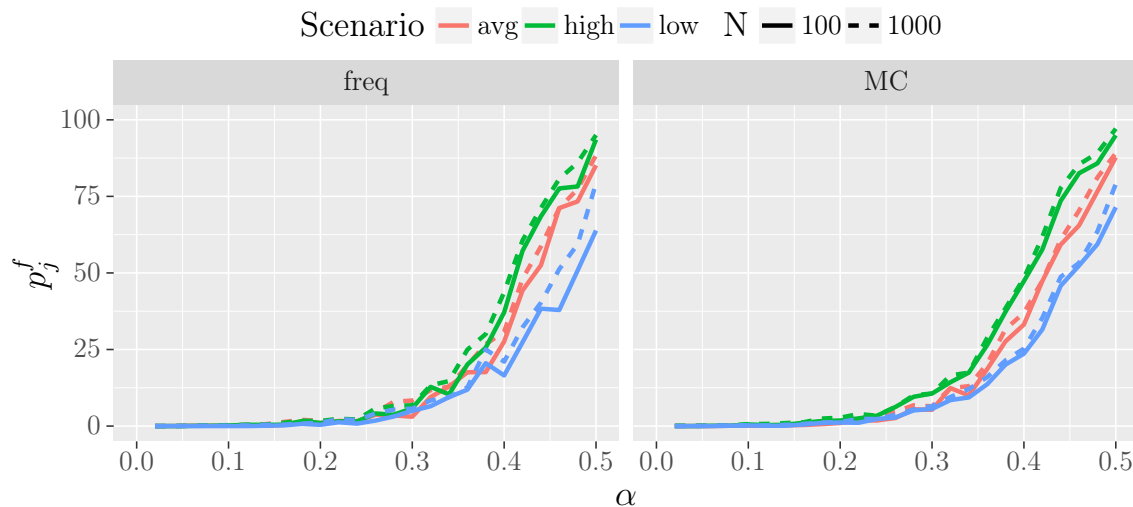


Figure 11: Effect of number of Monte-Carlo samples N on failure probability p_j^f of Reactor 1 (Instance P1¹⁹).

Both probability estimation approaches are dependent on the number N of operating mode sequences generated. Fig. 11 shows that increasing N from 100 to 1000 for Reactor 1 in Instance P1¹⁹ only has a small effect on p_j^f , especially for the Markov chain based approach. $N = 100$ is therefore deemed sufficient.

Figs. 12 and 13 compare Bayesian optimization (BO) with random search for Instance P1¹⁹. Overall cost (Eqn. 16) was evaluated over a horizon of 24 weeks and both Bayesian optimization and random search were repeated five times. For the Bayesian optimization, four points were sampled evenly from the interval $\alpha \in [0.02, 0.5]$ initially. Fig. 12 shows the obtained objective values as a function of α . There is clearly a trade-off between high cost of preventive maintenance in conservative solutions (small α) and high cost of corrective maintenance for less conservative but also less robust solutions (large α). Bayesian optimization very efficiently samples

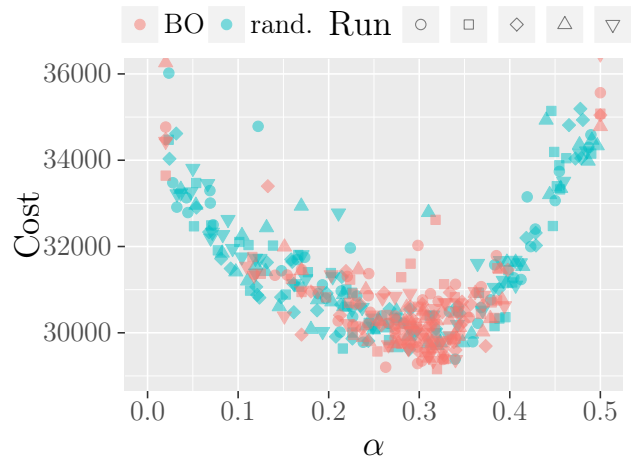


Figure 12: Bayesian optimization vs. random search. Five runs of BO and random search were conducted. BO efficiently explores values near the optimal α .

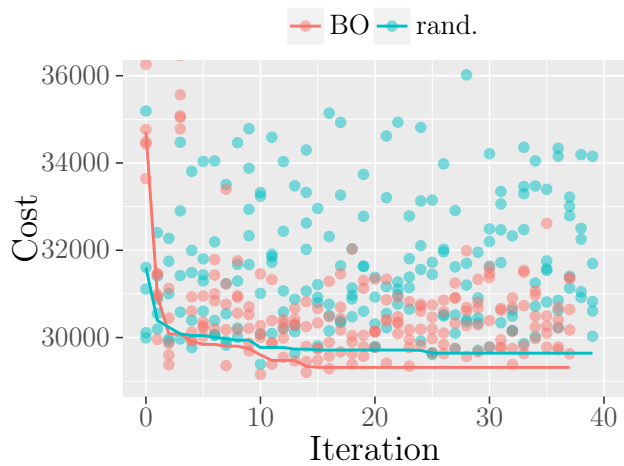


Figure 13: Bayesian optimization vs. random search. Points are individual values obtained at a given iteration. Lines represent the best previously achieved solution value averaged over five runs. BO consistently finds better solutions.

from the area around the optimal $\alpha \approx 0.3$ while random search naturally samples from the entire interval. Fig 13 shows the lowest objective value previously obtained as a function of the number of samples (averaged over five runs). Bayesian optimization consistently finds lower cost solutions than random search and achieves a good compromise between preventive and corrective maintenance within about 20 iterations.

6 Conclusion

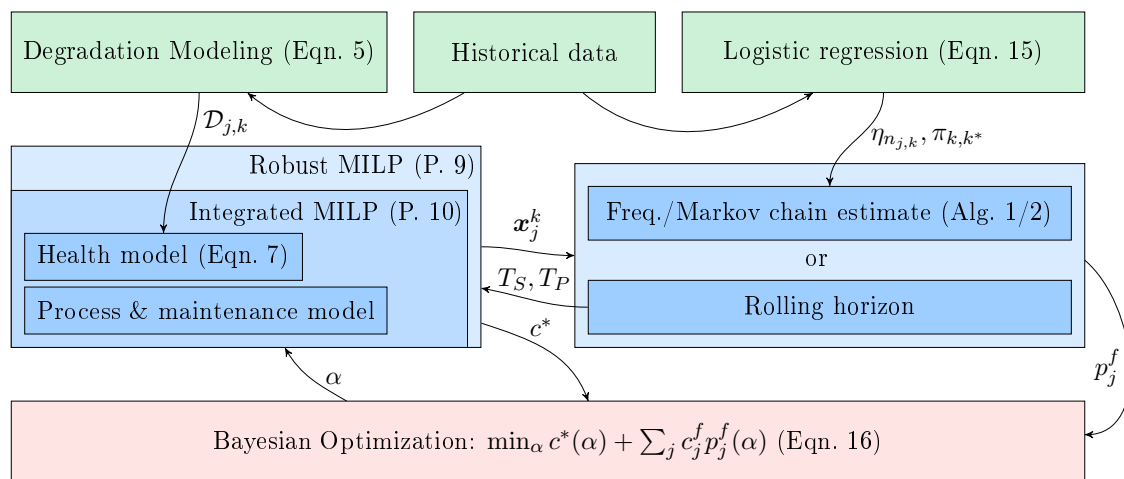


Figure 14: Flowchart of the proposed method.

This work integrates equipment degradation effects in process level optimization problems. The demonstrated methodology is summarized in Fig. 14. We combine commonly used methods from the Degradation Modeling literature, which allow unit health characteristics to be estimated and updated from data, with Robust Optimization. This is highly relevant since, realistically, almost all equipment in chemical and manufacturing processes will be subject to performance degradation and failures.

Solving realistic integrated maintenance and production scheduling and planning problems is a hard task by itself, because models tend to be large and computationally expensive. Combining such models with robust optimization increases the need for solving problems efficiently. Furthermore, the scheduling task is highly repetitive and should become easier as historical data is collected. To reduce computational

expense, we show conditions where robust optimization problems can be solved by solving a deterministic approximation and develop data-based methods for estimating failure probabilities.

In the context of computationally expensive models, we show that Bayesian Optimization can be used effectively to optimize the uncertainty set in Robust optimization and balance the trade-off between preventive and corrective maintenance.

7 Acknowledgement

This work was funded by the Engineering & Physical Sciences Research Council (EPSRC) Center for Doctoral Training in High Performance Embedded and Distributed Systems (EP/L016796/1), an EPSRC/Schlumberger CASE studentship to J.W. (EP/R511961/1, voucher 17000145), and an EPSRC Research Fellowship to R.M. (EP/P016871/1).

A Formulating the robust counterpart

The reformulation of the semi-infinite constraints

$$m_{j,t}s_j^0 \leq s_{j,t} \quad \forall t, j \in J, \tilde{d}_{j,k} \in \mathcal{D} \quad (22a)$$

$$s_{j,t} \leq s_j^{max} + m_{j,t} \cdot (s_j^0 - s_j^{max}) \quad \forall t, j \in J, \tilde{d}_{j,k} \in \mathcal{U} \quad (22b)$$

$$s_{j,t} \geq s_{j,t-\Delta t} + \sum_k x_{j,k,t} \tilde{d}_{j,k} + m_{j,t} \cdot (s_j^0 - s_j^{max}) \quad \forall t, j \in J, \tilde{d}_{j,k} \in \mathcal{U} \quad (22c)$$

$$s_{j,t} \leq s_{j,t-\Delta t} + \sum_k x_{j,k,t} \tilde{d}_{j,k} \quad \forall t, j \in J, \tilde{d}_{j,k} \in \mathcal{U} \quad (22d)$$

into a deterministic robust counterpart in this work is based on the approach by Lappas and Gounaris²⁵. $s_{j,t}$ is replaced by the affine decision rule

$$s_{j,t} = [s_{j,t}]_0 + \sum_k [s_{j,t}]_k \tilde{d}_{j,k}$$

in all constraints, where $[s_{j,t}]_0$ and $[s_{j,t}]_k$ are coefficients which become new variables in the reformulated constraints. The first constraint (Eqn. 22a) can be reformulate

in the following way:

$$\begin{aligned}
m_{j,t}s_j^0 &\leq [s_{j,t}]_0 + \sum_k [s_{j,t}]_k \tilde{d}_{j,k} \\
&\Rightarrow - \sum_k [s_{j,t}]_k \tilde{d}_{j,k} \leq [s_{j,t}]_0 - m_{j,t}s_j^0 \\
&\Rightarrow \Theta^* \leq [s_{j,t}]_0 - m_{j,t}s_j^0,
\end{aligned}$$

where

$$\begin{aligned}
\Theta^* &= \max_{\tilde{d}_{j,k}} - \sum_k [s_{j,t}]_k \tilde{d}_{j,k} \\
\text{s.t.} \quad & - \tilde{d}_{j,k} \leq -\bar{d}_{j,k}(1 - \epsilon) \quad \forall k \\
& \tilde{d}_{j,k} \leq \bar{d}_{j,k}(1 + \epsilon) \quad \forall k.
\end{aligned}$$

The dual of this is

$$\begin{aligned}
\Theta^* &= \min_{u^{1,j,t}, l^{1,j,t}} \sum_k \bar{d}_{j,k} [(1 + \epsilon)u_k^{1,j,t} - (1 - \epsilon)l_k^{1,j,t}] \\
\text{s.t.} \quad & u_k^{1,j,t} - l_k^{1,j,t} \geq -[s_{j,t}]_k \quad \forall k,
\end{aligned}$$

with dual variables $u_k^{1,j,t}$ and $l_k^{1,j,t}$. Dropping the minimization leads to the final reformulation:

$$\begin{aligned}
\sum_k \bar{d}_{j,k} [(1 + \epsilon)u_k^{1,j,t} - (1 - \epsilon)l_k^{1,j,t}] &\leq [s_{j,t}]_0 - m_{j,t}s_j^0 \quad \forall t, j \in J \\
u_k^{1,j,t} - l_k^{1,j,t} &\geq -[s_{j,t}]_k \quad \forall j, t, k
\end{aligned}$$

Similar analysis for the second inequality (Eqn. 22b) leads to reformulation

$$\begin{aligned}
&\sum_k \bar{d}_{j,k} [(1 + \epsilon)u_k^{2,j,t} - (1 - \epsilon)l_k^{2,j,t}] \\
&\leq s_j^{max} - [s_{j,t}]_0 + m_{j,t} \cdot (s_j^0 - s_j^{max}) \quad \forall t, j \in J \\
u_k^{2,j,t} - l_k^{2,j,t} &\geq [s_{j,t}]_k \quad \forall j, t, k,
\end{aligned}$$

the third inequality (Eqn. 22c) yields

$$\begin{aligned}
&\sum_k \bar{d}_{j,k} [(1 + \epsilon)u_k^{3,j,t} - (1 - \epsilon)l_k^{3,j,t}] \\
&\leq [s_{j,t}]_0 - [s_{j,t-\Delta t}]_0 + m_{j,t}s_j^{max} \quad \forall t, j \in J \\
u_k^{3,j,t} - l_k^{3,j,t} &\geq [s_{j,t-\Delta t}]_k - [s_{j,t}]_k + x_{j,k,t} \quad \forall j, t, k,
\end{aligned}$$

and the fourth (Eqn. 22d)

$$\begin{aligned}
& \sum_k \bar{d}_{j,k} [(1 + \epsilon)u_k^{4,j,t} - (1 - \epsilon)l_k^{4,j,t}] \\
& \leq -[s_{j,t}]_0 + [s_{j,t-\Delta t}]_0 \quad \forall t, j \in J \\
& u_k^{4,j,t} - l_k^{4,j,t} \geq -[s_{j,t-\Delta t}]_k + [s_{j,t}]_k - x_{j,k,t} \quad \forall j, t, k.
\end{aligned}$$

B Equivalence to deterministic optimization with maximal parameters

Note that for convenience and readability the index j has been dropped in all equations in this appendix.

Consider the case where the cost, process model, and maintenance model in Problem 9 are not functions of the uncertain parameters \tilde{d}_k :

$$\min_{\mathbf{x}, \mathbf{m}} \text{cost}(\mathbf{x}, \mathbf{m}) \quad (23a)$$

$$\text{s.t. process model}(\mathbf{x}, \mathbf{m}) \quad (23b)$$

$$\text{maintenance model}(\mathbf{x}, \mathbf{m}) \quad (23c)$$

$$m_t s_0 \leq [s_t]_0 + \sum [s_t]_k \tilde{d}_k, \quad \forall t, \tilde{d}_k \in \mathcal{U} \quad (23d)$$

$$[s_t]_0 + \sum [s_t]_k \tilde{d}_k \leq s^{max} + m_t (s^0 - s^{max}), \quad \forall t, \tilde{d}_k \in \mathcal{U} \quad (23e)$$

$$\begin{aligned}
[s_t]_0 + \sum [s_t]_k \tilde{d}_k & \geq [s_{t-1}]_0 + \sum [s_{t-1}]_k \tilde{d}_k \\
& + \sum_k x_{k,t} \tilde{d}_k \quad \forall t, \tilde{d}_k \in \mathcal{U} \quad (23f) \\
& + m_t (s^0 - s^{max}),
\end{aligned}$$

$$[s_t]_0 + \sum [s_t]_k \tilde{d}_k [s_{t-1}]_0 + \sum [s_{t-1}]_k \tilde{d}_k + \sum_k x_{k,t-1} \tilde{d}_k, \quad \forall t, \tilde{d}_k \in \mathcal{U} \quad (23g)$$

Furthermore consider a deterministic version of Problem 23

$$\min_{\mathbf{x}, \mathbf{m}} \text{cost}(\mathbf{x}, \mathbf{m}) \quad (24a)$$

$$\text{s.t. process model}(\mathbf{x}, \mathbf{m}) \quad (24b)$$

$$\text{maintenance model}(\mathbf{x}, \mathbf{m}) \quad (24c)$$

$$m_t s^0 \leq s_t, \quad \forall t \quad (24d)$$

$$s_t \leq s^{max} + m_t (s^0 - s^{max}), \quad \forall t \quad (24e)$$

$$s_t \geq s_{t-1} + \sum_k x_{k,t} d_k^{max} + m_t(s^0 - s^{max}), \quad \forall t \quad (24f)$$

$$s_t \leq s_{t-1} + \sum_k x_{k,t} d_k^{max}, \quad \forall t \quad (24g)$$

in which \tilde{d}_k has been replaced by

$$d_k^{max} = \max_{\tilde{d}_k \in \mathcal{U}} \tilde{d}_k.$$

Theorem 2. *Given that cost, process model, and maintenance model are not functions of $\tilde{d}_{j,k}$ and that $s_j^0 \leq s_j^{init} = s_{j,t=t_0} \leq s_j^{max}$ and $\tilde{d}_{j,k} \geq 0, \forall \tilde{d}_{j,k} \in \mathcal{U}$, then a feasible solution $(\mathbf{x} = [x_{k,t}, \dots], \mathbf{m} = [m_t, \dots], \mathbf{h} = [s_t])$ to Problem 24 forms a feasible solution $(\mathbf{x} = [x_{k,t}, \dots], \mathbf{m} = [m_t, \dots], \mathbf{h} = [[s_t]_0, [s_t]_k])$ to Problem 23 with*

$$[s_t]_0 = \begin{cases} s^{init} & t < t_{m,0} \\ s^0 & t \geq t_{m,0} \end{cases} \quad (25a)$$

$$[s_t]_k = \sum_{t'=t_{m,t}}^t x_{k,t'}, \quad (25b)$$

where $s^{init} = s(t=0)$, $t_{m,0}$ is the first point in time at which maintenance is performed, and $t_{m,t}$ is the most recent point in time at which maintenance was performed.

Proof. First we show that the Inequality 23d

$$m_t s^0 \leq [s_t]_0 + \sum [s_t]_k \tilde{d}_k \quad (23d)$$

holds for any $\tilde{d}_k \geq 0$ given $(\mathbf{x} = [x_{k,t}, \dots], \mathbf{m} = [m_t, \dots], \mathbf{h} = [[s_t]_0, [s_t]_k])$: From the assumption $s^0 \leq s^{init} \leq s^{max}$ and Eqn. 25a it follows that $s^0 \leq [s_t]_0 \leq s^{max}$. Furthermore, it directly follows from Eqn. 25b that $[s_t]_k \geq 0$. Eqn. 23d is therefore guaranteed to hold for any $\tilde{d}_k \in \mathcal{U}, \tilde{d}_k \geq 0$.

Next, we show that Inequalities 23f and 23g,

$$[s_t]_0 + \sum [s_t]_k \tilde{d}_k \geq [s_{t-1}]_0 + \sum [s_{t-1}]_k \tilde{d}_k + \sum_k x_{k,t} \tilde{d}_k + m_t(s^0 - s^{max}) \quad (23f)$$

and

$$[s_t]_0 + \sum [s_t]_k \tilde{d}_k \leq [s_{t-1}]_0 + \sum [s_{t-1}]_k \tilde{d}_k + \sum_k x_{k,t} \tilde{d}_k \quad (23g)$$

respectively, hold for any $\tilde{d}_k \in \mathcal{U}$ as long as Inequality 23e is satisfied. We first assume that $m_t = 0$. In this case $[s_t]_k = [s_{t-1}]_k + x_{k,t}$ (from Eqn. 25b), $[s_t]_0 = [s_{t-1}]_0$ (from Eqn. 25a) and Eqns. 23f and 23g simplify to

$$[s_t]_0 \geq [s_{t-1}]_0$$

and

$$[s_t]_0 \leq [s_{t-1}]_0,$$

which is true for any \tilde{d}_k . Next we assume that $m_t = 1$. In this case $[s_t]_0 = s^0$ (from Eqn. 25a), $[s_t]_k = 0$ (from Eqn. 25b), and $x_{k,t} = 0$ (assuming that a unit can not be operated while maintenance is performed). Substituting this into Eqns. 23f and 23g and rearranging yields

$$[s_{t-1}]_0 + \sum [s_{t-1}]_k \tilde{d}_k \leq s^{max} \quad (26)$$

and

$$s^0 \leq [s_{t-1}]_0 + \sum [s_{t-1}]_k \tilde{d}_k \quad (27)$$

respectively. Eqn. 26 is guaranteed to be satisfied as long as Inequality 23e holds for $t = t - 1$ and Eqn. 27 holds for any $\tilde{d}_k \in \mathcal{U}$, $\tilde{d}_k \geq 0$ since $[s_{t-1}]_0 \geq S_0$ and $[s_{t-1}]_k \geq 0$.

Finally we show that the Inequality 23e

$$[s_t]_0 + \sum [s_t]_k \tilde{d}_k \leq s^{max} + m_t(s^0 - s^{max}) \quad (23e)$$

holds for any $\tilde{d}_k \in \mathcal{U}$. To this end we notice that

$$\arg \max_{\tilde{d}_k \in \mathcal{U}} [s_t]_0 + \sum [s_t]_k \tilde{d}_k = d_k^{max}$$

since $[s_t]_k \geq 0$. Therefore, if Eqn. 23e holds for $\tilde{d}_k = d_k^{max}$, it holds for any $\tilde{d}_k \in \mathcal{U}$. Since $(\mathbf{x} = [x_{k,t}, \dots], \mathbf{m} = [m_t, \dots], \mathbf{h} = [s_t])$ is a solution to Problem 24,

$$s_t \leq s^{max} + m_t(s^0 - s^{max}). \quad (28)$$

Lastly, noticing that the definition of $[s_t]_0$ and $[s_t]_k$ (Eqns. 25a and 25b) ensure that s_t can always be decomposed as

$$s_t = [s_t]_0 + \sum [s_t]_k d_k^{max}$$

if s_t satisfies Problem 24, it follows that

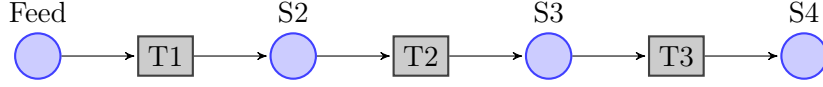
$$s_t = [s_t]_0 + \sum [s_t]_k d_k^{max} \leq s^{max} + m_t(s^0 - s^{max})$$

and Eqn. 23e holds for all $\tilde{d}_k \in \mathcal{U}$. □

C Instances of the STN

States	Feed A	Feed B	Feed C	Hot A	Int. BC	Int. AB	Impure E	Prod. 1	Prod. 2
Capacity [kg]	∞	∞	∞	100	200	150	100	∞	∞
Initial [kg]	∞	∞	∞	0	0	0	0	0	0
Storage cost	0	0	0	1	1	1	1	5	5
Units	Heater	Reactor 1	Reactor 2	Still					
v_j^{min} [kg]	40	32	20	80					
v_j^{max} [kg]	100	80	50	200					
s_j^{max}	80	150	160	100					
s_j^{init}	30	50	120	40					
τ_j [hr]	15	21	24	15					
c_j^{maint}	300	900	2000	1200					
c_j^f	2000	3000	3000	1500					
Task	Mode	Unit							
		Heater		Reactor 1		Reactor 2		Still	
		$p_{i,j,k}$	$d_{i,j,k}/\sigma_{i,j,k}$	p	d/σ	p	d/σ	p	d/σ
Heating	Slow	9	1/0.27						
	Normal	6	2/0.54						
	Fast	3	3/0.81						
Reaction 1	Slow			27	4/1.08	30	4/1.08		
	Normal			15	5/1.35	18	5/1.35		
	Fast			8	8/2.43	12	10/2.7		
Reaction 2	Slow			36	1/0.27	33	2/0.54		
	Normal			21	3/0.81	18	4/1.08		
	Fast			15	5/1.35	12	4/1.08		
Reaction 3	Slow			30	3/0.81	24	2/0.54		
	Normal			18	7/1.89	21	5/1.35		
	Fast			6	8/2.16	12	9/2.43		
Separation	Slow							15	2/0.54
	Normal							9	5/1.35
	Fast							6	6/1.62
Period	Scenario								
	Low		Average		High				
	Product 1	Product 2	Product 1	Product 2	Product 1	Product 2			
1	76	136	150	200	190	294			
2	116	162	88	150	231	323			
3	101	115	125	197	198	307			
4	91	141	67	296	217	335			
5	60	147	166	191	181	293			
6	60	103	203	193	244	328			
7	54	148	90	214	243	326			
8	110	113	224	294	182	296			
9	92	105	174	247	246	296			
10	99	175	126	313	189	348			
11	51	177	66	226	199	319			
12	117	164	119	121	222	346			
13	108	124	234	197	246	331			
14	64	107	64	242	239	336			
15	62	154	103	220	180	302			
16	62	135	77	342	216	306			
17	71	109	132	355	218	302			
18	86	139	186	320	213	349			
19	80	102	174	335	233	284			
20	70	172	239	298	191	347			
21	92	120	124	252	233	303			
22	59	153	194	222	181	303			
23	70	124	91	324	189	307			
24	75	141	228	337	188	299			

Table 3: Instance P1¹⁹



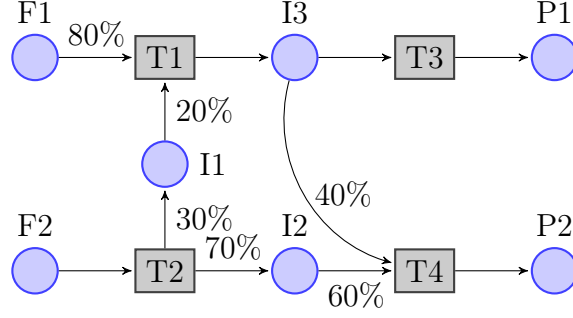
States		S1	S2	S3	S4
Capacity [kg]		∞	∞	∞	∞
Initial [kg]		∞	0	0	0
Storage cost		0	1	1	1

Units		U1	U2	U3	U4	U5
v_j^{min} [kg]		0	0	0	0	0
v_j^{max} [kg]		100	150	200	150	150
s_j^{max}		120	100	150	90	80
s_j^{mit}		10	70	45	60	30
t_j [hr]		21	15	18	9	13
c_j^{maint}		600	600	500	400	400

Task	Mode	Unit									
		U1		U2		U3		U4		U5	
		$p_{i,j,k}$	$\bar{d}_{i,j,k}/\sigma_{i,j,k}$	p	d/σ	p	d/σ	p	d/σ	p	d/σ
T1	Slow	33	3/0.66	30	3/0.66						
T1	Normal	25	5/1.35	21	6/1.62						
T1	Fast	15	7/2.17	12	9/2.79						
T2	Slow					24	4/0.88				
T2	Normal					18	6/1.62				
T2	Fast					12	10/3.1				
T3	Slow							21	2/0.44	18	2/0.44
T3	Normal							15	4/1.08	12	4/1.08
T3	Fast							9	7/2.17	6	6/1.86

Period	Scenario			Period	Scenario		
	Low	Average	High		Low	Average	High
1	725	1167	2002	13	446	947	1847
2	587	1110	2141	14	201	1426	2178
3	397	1087	1668	15	305	1090	2159
4	558	906	1977	16	447	1040	2015
5	411	1188	1692	17	378	917	1662
6	678	1191	1805	18	566	1190	1782
7	252	1436	2007	19	409	953	1646
8	415	1020	2174	20	797	1109	2135
9	539	1110	1713	21	605	1298	2113
10	414	1266	2162	22	413	1275	1760
11	214	1042	2155	23	550	1364	1958
12	612	1169	2018	24	362	1158	1779

Table 4: Instance P2²⁶



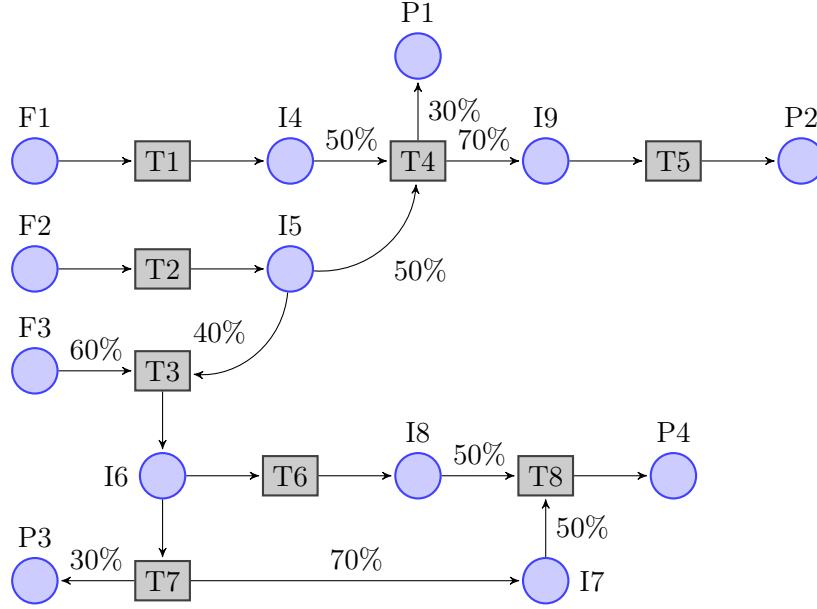
States	F1	F2	I1	I2	I3	P1	P2
Capacity [kg]	∞	∞	200	100	500	1000	1000
Initial [kg]	∞	∞	0	0	0	0	0
Storage cost	0	0	1	1	1	5	5

Units	R1	R2	R3
v_j^{min} [kg]	40	25	40
v_j^{max} [kg]	80	50	80
s_j^{max}	70	120	70
s_j^{init}	10	10	10
τ_j [hr]	21	21	21
c_j^{maint}	600	600	600

Task	Mode	Unit					
		R1		R2		R3	
		$p_{i,j,k}$	$d_{i,j,k}/\sigma_{i,j,k}$	p	d/σ	p	d/σ
T1	Slow	24	3/0.66	24	3/0.66		
T1	Normal	15	5/1.35	15	5/1.35		
T1	Fast	9	8/2.16	9	8/2.16		
T2	Slow	36	3/0.66	36	3/0.66		
T2	Normal	24	5/1.35	24	5/1.35		
T2	Fast	15	8/2.16	15	8/2.16		
T3	Slow					12	3/0.66
T3	Normal					9	5/1.35
T3	Fast					6	8/2.16
T4	Slow					24	3/0.66
T4	Normal					15	5/1.35
T4	Fast					9	8/2.16

Period	Scenario						Period	Scenario					
	Low		Average		High			Low		Average		High	
	P1	P2	P1	P2	P1	P2		P1	P2	P1	P2	P1	P2
1	190	102	271	231	311	305	13	197	192	213	280	314	376
2	172	156	230	282	381	347	14	120	100	257	270	370	392
3	102	103	274	226	381	321	15	180	115	286	223	335	370
4	130	172	289	281	310	310	16	178	186	201	281	386	358
5	130	104	270	212	317	371	17	135	138	288	289	398	309
6	174	192	205	205	339	328	18	140	115	284	253	304	396
7	167	194	260	248	379	348	19	128	104	200	273	334	351
8	185	175	259	282	317	392	20	155	179	275	210	326	300
9	179	180	211	233	300	387	21	158	120	298	253	315	397
10	131	120	261	292	346	326	22	160	186	252	284	301	396
11	104	196	271	212	364	364	23	125	105	223	220	396	378
12	104	188	202	289	309	346	24	187	134	205	285	316	393

Table 5: Instance P4²⁷



States	F1	F2	F3	I4	I5	I6	I7	I8	I9	P1	P2	P3	P4
Capacity [kg]	∞	∞	∞	1000	1000	1500	2000	1000	3000	∞	∞	∞	∞
Initial [kg]	∞	∞	∞	0	0	0	0	0	0	0	0	0	0
Storage cost	0	0	0	1	1	1	1	1	1	5	5	5	5

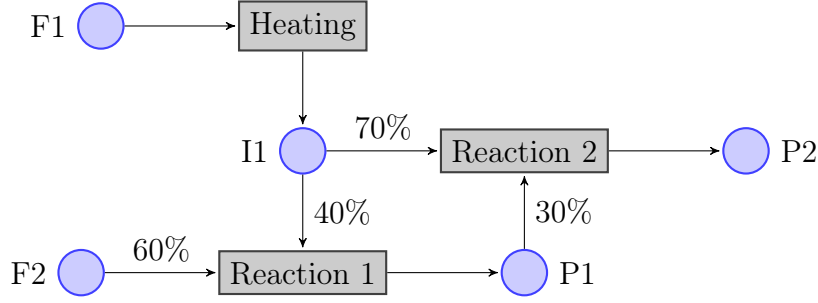
Units	R1	R2	R3	R4	R5	R6
v_j^{min} [kg]	0	0	0	0	0	0
v_j^{max} [kg]	1000	2500	3500	1500	1000	4000
s_j^{max}	100	100	100	100	100	100
s_j^{init}	77	80	90	17	40	33
τ_j [hr]	21	21	21	21	21	21
c_j^{maint}	1000	1700	2000	1200	1000	2100

Task	Mode	Unit											
		R1		R2		R3		R4		R5		R6	
		$p_{i,j,k}$	$d_{i,j,k}/\sigma_{i,j,k}$	p	d/σ	p	d/σ	p	d/σ	p	d/σ	p	d/σ
T1	Slow	18	3/0.66										
T1	Normal	12	5/1.35										
T2	Slow							24	3/0.66				
T2	Normal							15	5/1.35				
T3	Slow			33	5/0.66								
T3	Normal			21	8/1.35								
T4	Slow					42	5/0.66						
T4	Normal					21	11/1.35						
T5	Slow											45	7/0.66
T5	Normal											30	10/1.35
T6	Slow									18	3/0.66		
T6	Normal									12	5/1.35		
T7	Slow			33	6/0.66								
T7	Normal			21	9/1.35								
T8	Slow											45	6/0.66
T8	Normal											30	10/1.35

Table 6: Instance P6²⁸

Period	Scenario											
	Low				Average				High			
	P1	P2	P3	P4	P1	P2	P3	P4	P1	P2	P3	P4
1	715	501	801	933	1277	1356	1739	1349	1605	1844	1898	1631
2	593	878	888	739	1533	1361	1384	1374	1687	1882	1650	1732
3	743	995	817	563	1727	1400	1323	1351	1510	1805	1893	1699
4	620	963	636	698	1702	1701	1260	1605	1557	1717	1693	1908
5	991	612	535	686	1521	1424	1600	1315	1929	1769	1657	1918
6	919	819	914	626	1451	1412	1667	1406	1539	1818	1676	1521
7	648	799	920	549	1447	1471	1732	1620	1999	1663	1632	1603
8	609	728	969	925	1746	1444	1694	1512	1673	1987	1924	1742
9	741	575	604	814	1691	1456	1384	1305	1826	1559	1982	1882
10	968	682	853	532	1436	1297	1564	1356	1987	1737	1598	1910
11	624	789	816	728	1357	1730	1441	1638	1696	1660	1761	1778
12	840	929	700	733	1384	1283	1461	1423	1779	1722	1558	1655
13	516	790	705	743	1387	1594	1696	1533	1596	1528	1857	1745
14	556	643	974	890	1722	1493	1528	1533	1782	1829	1994	1512
15	940	715	797	638	1470	1377	1635	1303	1949	1738	1933	1782
16	894	896	693	853	1563	1467	1526	1565	1837	1593	1938	1852
17	792	994	509	647	1561	1593	1614	1531	1694	1869	1879	1593
18	725	718	856	789	1739	1681	1373	1255	1902	1663	1814	1953
19	820	886	971	531	1576	1706	1635	1628	1875	1988	1648	1512
20	950	788	580	859	1627	1358	1469	1694	1642	1519	1999	1595
21	641	773	681	877	1257	1433	1581	1420	1890	1942	1854	1826
22	793	963	950	634	1250	1641	1644	1404	1795	1628	1658	1961
23	504	741	531	671	1472	1617	1311	1519	1967	1768	1877	1739
24	830	529	819	594	1390	1645	1632	1614	1844	1945	1620	1563

Table 7: Instance P6²⁸ continued



States	F1	F2	I1	P1	P2								
Capacity [kg]	∞	∞	∞	∞	∞								
Initial [kg]	∞	∞	0	0	0								
Storage cost	0	0	15	9	5								
Units	Heater		Reactor										
v_j^{min} [kg]	40	30											
v_j^{max} [kg]	100	140											
s_j^{max}	80	120											
s_j^{init}	43	30											
τ_j [hr]	2	3											
c_j^{maint}	300	300											
Task	Mode	Unit											
		Heater		Reactor									
		$p_{i,j,k}$	$d_{i,j,k}/\sigma_{i,j,k}$	p	d/σ								
Heating	Slow	9	5.5/1.49										
Heating	Normal	6	11/2.97										
Reaction 1	Slow			6	7/1.89								
Reaction 1	Normal			4	9/2.43								
Reaction 2	Slow			10	5/1.35								
Reaction 2	Normal			6	13/3.51								
Period	Scenario						Period	Scenario					
	Low		Average		High			Low		Average		High	
	P1	P2	P1	P2	P1	P2		P1	P2	P1	P2	P1	P2
1	52	61	121	113	184	201	13	49	45	141	128	180	225
2	60	32	137	149	228	207	14	29	44	115	120	210	192
3	42	59	149	128	204	218	15	69	35	148	106	220	192
4	51	40	146	127	192	200	16	53	51	125	148	224	225
5	24	42	105	103	206	225	17	38	49	102	136	229	218
6	34	52	111	100	194	212	18	47	77	112	125	204	201
7	32	55	105	143	223	216	19	54	53	141	134	197	226
8	30	62	141	140	182	218	20	26	77	118	131	223	215
9	65	30	144	128	185	197	21	61	68	116	128	199	183
10	32	69	147	122	218	180	22	31	71	132	101	212	196
11	59	37	119	119	182	197	23	53	42	107	121	181	222
12	24	44	133	139	218	195	24	39	47	113	143	220	211

Table 8: Toy instance

Except for the toy instance, all instances are taken from the benchmark collection by Lappas and Gounaris²⁵. All parameters were converted to a discrete time formulation and degradation parameters were added. For Instance P1¹⁹ parameters from Biondi et al.¹⁸ were used. The time steps and horizons used in each instance are given in Table 9.

Instance	Toy	P1 ¹⁹	P2 ²⁶	P4 ²⁷	P6 ²⁸
T_S	30	168	168	168	168
Δt_S	1	3	3	3	3
T_P	720	4032	4032	4032	4032
Δt_P	30	168	168	168	168

Table 9: Time horizons of STN instances

The degradation of all units is assumed to follow a Wiener process. The distribution of increments is

$$S_{j,t+p_{i,j,k}} - S_{j,t} = D_{i,j,k}, \quad D_{i,j,k} \sim \mathcal{N}(\bar{d}_{i,j,k}, \sigma_{i,j,k}^2),$$

where $\bar{d}_{i,j,k}$ is the nominal amount of degradation when task i is performed on unit j in mode k . When no task is being processed the degradation signal is assumed to vary with zero mean and a small variance:

$$S_{j,t+\Delta t} - S_{j,t} = D_{0,\Delta t}, \quad D_{0,\Delta t} \sim \mathcal{N}(0, 0.05^2 \Delta t). \quad (29)$$

A detailed list of all parameter values used in each case study can be found in Tables 3 through 8.

D Crossing probabilities of a Brownian motion for a piecewise linear boundary

When the Wiener process is used as a degradation model, the failure probability p_j^f can be calculated efficiently based on analytical result^{44,45,63}. The probability of a Wiener process with piecewise constant parameters $\theta_{j,k} = [\mu_{j,k}, \sigma_{j,k}]$ crossing a fixed threshold s_j^{max} is equivalent to the probability of a standard Brownian motion $W(t)$ (a Wiener process with $\mathcal{N}(0, 1)$ distributed increments) crossing a piecewise linear boundary. The probability of $W(t)$ crossing a linear boundary $at + b$ is known to be inverse gaussian distributed

$$P(W(t) \geq at + b, t \leq T) = 1 - \Phi\left(\frac{aT + b}{\sqrt{T}}\right) + \exp^{-2ab} \Phi\left(\frac{aT - b}{\sqrt{T}}\right), \quad (30)$$

where $\Phi(\cdot)$ is the standard normal distribution function⁶⁴.

Based on this, the probability of failure $p_j^{u,v}$ between two consecutive maintenance times $t_{m,u}$ and $t_{m,v}$ can be calculated as

$$\begin{aligned} p_j^{u,v} &= 1 - \mathbb{E}h(\mathbf{y}) \\ &= 1 - \prod_{l=1}^n \mathbb{1}(y_l > 0) \left(1 - \exp \left[-\frac{2y_{l-1}y_l}{t_l - t_{l-1}} \right] \right), \end{aligned}$$

where $t_l, l \in \{1, \dots, n\}$ are the n points in time between $t_{m,u}$ and $t_{m,v}$ at which the operating mode k changes⁴⁴.

Here \mathbf{y} is a vector representing the values of $W(t)$ at each t_l . It is defined as

$$\mathbf{y} = \mathbf{c} + \mathbf{M}\mathbf{D}^{1/2}\mathbf{u},$$

where \mathbf{M} is a lower triangular matrix of ones,

$$\mathbf{D}^{1/2} = \text{diag}(\sqrt{t_1 - t_{m,u}}, \sqrt{t_2 - t_1}, \dots, \sqrt{t_{m,v} - t_n}),$$

\mathbf{u} is a random vector with $u_l \sim \mathcal{N}(0, \sigma_{j,k}^2(t_l))$, and \mathbf{c} is the piecewise linear boundary

$$\mathbf{c} = (s_j^{max} - s_j^{init}) \cdot [1, \dots, 1]^\top - \mathbf{M} \text{diag}(0, \mu_{j,k}(t_1), \dots, \mu_{j,k}(t_n)) \Delta \mathbf{t}$$

with

$$\Delta \mathbf{t} = [0, t_1 - t_0, \dots, t_n - t_{n-1}]^\top.$$

The overall probability of failure over the evaluation horizon T can then be calculated as

$$p_j^f = 1 - \prod_{u=1}^{n+1} (1 - p_j^{u-1,l}), \quad (31)$$

where $t_{m,0} = 0$, $t_{m,n+1} = T$, and $t_{m,u}, u \in \{1, \dots, n\}$ are the n points in time at which maintenance is carried out on unit j in the evaluation horizon.

E Nomenclature

\mathbf{h}	health variables
\mathbf{m}	maintenance variables
\mathbf{x}	process variables

Indices

i	task
j	unit
k	operating mode
s	state
t	time

Sets

I	set of tasks
I_j	set of tasks i available on unit j
I_s	set of tasks i consuming state s
\bar{I}_s	set of tasks i producing state s
J	set of process units
J_i	set of units j on which task i can be performed
K_i	set of operating modes allowed for task i
K_j	set of operating modes k available on unit j
T	evaluation horizon
T_P	planning horizon
T_S	scheduling horizon
\mathcal{U}	uncertainty set
\mathcal{X}	set of operating mode sequences \mathbf{x}_j^k

Discrete Variables

$m_{j,t}$	1 if maintenance is performed on unit j at time t
$n_{i,j,k,t}$	number of times task i is performed on unit j in mode k in time period t
$w_{i,j,k,t}$	1 if task i starts on unit j in mode k at time t , 0 otherwise
$x_{j,k,t}$	1 if unit j is operated in mode k at time t
\mathbf{x}_j^k	sequence of operating modes $[k_1, k_2, \dots, k_T]$
$\omega_{j,k,t}$	1 if unit j operates in mode k in period t , 0 otherwise

Continuous Variables

$a_{i,j,k,t}$	amount of material processed by task i in unit j in mode k in time period t
$b_{i,j,k,t}$	amount of material committed to task i on unit j in mode k at time t
c^*	minimal cost determined by solving Problem 9
c_j^f	cost of unit j failing
D	random variable modeling increment of $S(t)$
$N_{j,k}$	random variable modeling $n_{j,k}$

$n_{j,k}$	number of times mode k occurs on unit j in a given Δt
p_j^f	probability of failure
\bar{p}_j^f	estimated upper bound on p_j^f
q_s^{fin}	quantity of state s stored at end of planning horizon
$q_{s,t}$	quantity of state s stored at time t
$S(t)$	stochastic process modeling $s^{meas}(t)$
$s_{j,t}^n$	realization of $S_j(t)$ at time t
s_j^{fin}	value of degradation signal at end of planning horizon
$s^{meas}(t)$	measured degradation signal
S_t	random variable modeling $s^{meas}(t)$ at time t
$X_j^k(t)$	memoryless Markov chain modeling \mathbf{x}_j^k
$X_{j,t}^k$	state of Markov chain at time t
ϕ_s^d	slack variable for unfulfilled demand of state s
$\phi_{s,t}^q$	slack variable for storage capacity violation of state s at time t
ψ	process/environmental parameters

Parameters

c_j^{maint}	cost of maintenance for unit j
$c_s^{storage}$	per unit cost of storage for state s
c_s	storage capacity of state s
\mathcal{D}	distribution of D
$\bar{d}_{j,k}$	nominal value of $\tilde{d}_{j,k}$
$\tilde{d}_{j,k}$	uncertain parameter modeling increment of $S(t)$
$\tilde{d}_{j,k}^{max}$	maximum of $\tilde{d}_{j,k}$ in \mathcal{U}
N	number of samples in Monte-Carlo simulation
$p_{i,j,k}$	processing time of task i on unit j in mode k
$r_{j,t}$	residual lifetime of unit j at time t
$[s_{j,t}]_0, [s_{j,t}]_k$	parameters for affine decision rule
s^0	reset value degradation signal
s^{init}	initial value of degradation signal
s^{max}	failure threshold degradation signal
\bar{t}_P	first time period in planning horizon
\bar{t}_S	last time period in scheduling horizon
Δt_P	length of planning period
Δt_S	length of scheduling period
U	large number
$v_{i,j}^{max}$	maximum batch size for task i on unit j
$v_{i,j}^{min}$	minimum batch size for task i on unit j

α	size parameter of \mathcal{U}
$\delta_{s,t}$	demand for s at time t
$\epsilon_{j,k}$	size parameter of \mathcal{U}
$\eta_{j,k}$	probability of k occurring $n_{j,k}$ times
θ	parameter vector of \mathcal{D}
$\mu_{j,k}$	mean of $\mathcal{D}_{j,k}$
π_{k,k^*}	transition probability Markov chain
$\bar{\rho}_{i,s}$	fraction of state s of material produced by task i
$\rho_{i,s}$	fraction of state s of material consumed by task i
$\sigma_{j,k}$	standard deviation of $\mathcal{D}_{j,k}$
τ_j	duration of maintenance on unit j

References

- [1] Andrew K.S. Jardine, Daming Lin, and Dragan Banjevic. A review on machinery diagnostics and prognostics implementing condition-based maintenance. *Mechanical Systems and Signal Processing*, 20(7):1483–1510, 2006.
- [2] Diana Barraza-Barraza, Jorge Limón-Robles, and Mario G Beruvides. Opportunities and challenges in Condition-Based Maintenance research. *IIE Annual Conference and Expo 2014*, pages 3035–3043, 2014.
- [3] Alexandros Bousdekis, Babis Magoutas, Dimitris Apostolou, and Gregoris Mentzas. Review, analysis and synthesis of prognostic-based decision support methods for condition based maintenance. *Journal of Intelligent Manufacturing*, pages 1–14, 2015.
- [4] Suzan Alaswad and Yisha Xiang. A review on condition-based maintenance optimization models for stochastically deteriorating system. *Reliability Engineering & System Safety*, 157:54–63, 2017.
- [5] William Q. Meeker and Yili Hong. Reliability Meets Big Data: Opportunities and Challenges. *Quality Engineering*, 26(1):102–116, 2014.
- [6] Ilias T. Dedopoulos and Nilay Shah. Optimal Short-Term Scheduling of Maintenance and Production for Multipurpose Plants. *Industrial & Engineering Chemistry Research*, 34(1):192–201, 1995.
- [7] I.T. Dedopoulos and N. Shah. Preventive maintenance policy optimization for multipurpose plant equipment. *Computers & Chemical Engineering*, 19:693–698, 1995.

- [8] Constantinos Georgiou Vassiliadis. *Integration of Maintenance Optimization in Process Design and Operation under Uncertainty*. PhD thesis, Imperial College of Science, Technology and Medicine, 1999.
- [9] C.G. Vassiliadis and E.N. Pistikopoulos. Maintenance scheduling and process optimization under uncertainty. *Computers and Chemical Engineering*, 25(2-3): 217–236, 2001.
- [10] J. Casas-Liza, J.M. Pinto, and L.G. Papageorgiou. Mixed Integer Optimization for Cyclic Scheduling of Multiproduct Plants Under Exponential Performance Decay. *Chemical Engineering Research and Design*, 83(10):1208–1217, 2005.
- [11] Michael C. Georgiadis, Lazaros G. Papageorgiou, and Sandro Macchietto. Optimal Cleaning Policies in Heat Exchanger Networks under Rapid Fouling. *Industrial & Engineering Chemistry Research*, 39(2):441–454, 2000.
- [12] Songsong Liu, Ahmed Yahia, and Lazaros G. Papageorgiou. Optimal Production and Maintenance Planning of Biopharmaceutical Manufacturing under Performance Decay. *Industrial & Engineering Chemistry Research*, 53(44):17075–17091, 2014.
- [13] Dionysios P. Xenos, Georgios M. Kopanos, Matteo Ciccotti, and Nina F. Thornhill. Operational optimization of networks of compressors considering condition-based maintenance. *Computers and Chemical Engineering*, 84:117–131, 2016.
- [14] Nur I. Zulkaffi and Georgios M. Kopanos. Planning of production and utility systems under unit performance degradation and alternative resource-constrained cleaning policies. *Applied Energy*, 183:577–602, 2016.
- [15] Nur I. Zulkaffi and Georgios M. Kopanos. Integrated condition-based planning of production and utility systems under uncertainty. *Journal of Cleaner Production*, 167:776–805, 2017.
- [16] Adrian M. Aguirre and Lazaros G. Papageorgiou. Medium-term optimization-based approach for the integration of production planning, scheduling and maintenance. *Computers and Chemical Engineering*, 0:1–21, 2018.
- [17] Sreekanth Rajagopalan, Nikolaos V. Sahinidis, Satyajith Amaran, Anshul Agarwal, Scott J. Bury, Bikram Sharda, and John M. Wassick. Risk analysis of turnaround reschedule planning in integrated chemical sites. *Computers & Chemical Engineering*, 107:381–394, 2017.

- [18] Matteo Biondi, Guido Sand, and Iiro Harjunkoski. Optimization of multipurpose process plant operations: A multi-time-scale maintenance and production scheduling approach. *Computers and Chemical Engineering*, 99:325–339, 2017.
- [19] E. Kondili, C.C. Pantelides, and R.W.H. Sargent. A general algorithm for short-term scheduling of batch operations - I. MILP formulation. *Computers and Chemical Engineering*, 17(2):211–227, 1993.
- [20] Murat Yildirim, Xu Andy Sun, and Nagi Z Gebraeel. Sensor-Driven Condition-Based Generator Maintenance Scheduling - Part I: Maintenance Problem. *IEEE Transactions on Power Systems*, 31(6):4253–4262, 2016.
- [21] Murat Yildirim, Xu Andy Sun, and Nagi Z Gebraeel. Sensor-Driven Condition-Based Generator Maintenance Scheduling - Part II: Incorporating Operations. *IEEE Transactions on Power Systems*, 31(6):4263–4271, 2016.
- [22] Murat Yildirim, Nagi Z. Gebraeel, and Xu Andy Sun. Integrated Predictive Analytics and Optimization for Opportunistic Maintenance and Operations in Wind Farms. *IEEE Transactions on Power Systems*, 32(6):4319–4328, 2017.
- [23] Beste Başçiftci, Shabbir Ahmed, Nagi Z. Gebraeel, and Murat Yildirim. Stochastic Optimization of Maintenance and Operations Schedules under Unexpected Failures. *IEEE Transactions on Power Systems*, 8950(c):1–1, 2018.
- [24] Adriaen Verheyleweghen and Johannes Jäschke. Framework for Combined Diagnostics, Prognostics and Optimal Operation of a Subsea Gas Compression System. *IFAC-PapersOnLine*, 50(1):15916–15921, 2017.
- [25] Nikolaos H Lappas and Chrysanthos E Gounaris. Multi-stage adjustable robust optimization for process scheduling under uncertainty. *AIChE Journal*, 62(5):1646–1667, 2016.
- [26] Iftekhar A. Karimi and Conor M. McDonald. Planning and Scheduling of Parallel Semicontinuous Processes. 2. Short-Term Scheduling. *Industrial & Engineering Chemistry Research*, 36(7):2701–2714, 1997.
- [27] Christos T. Maravelias and Ignacio E. Grossmann. New general continuous-time state - Task network formulation for short-term scheduling of multipurpose batch plants. *Industrial & Engineering Chemistry Research*, 42(13):3056–3074, 2003.

- [28] M. G. Ierapetritou and C. A. Floudas. Effective continuous-time formulation for short-term scheduling. 1. Multipurpose batch processes. *Industrial & Engineering Chemistry Research*, 37(11):4341–4359, 1998.
- [29] Peng Wang and David Coit. Reliability and Degradation Modeling with Random or Uncertain Failure Threshold. In *2007 Proceedings - Annual Reliability and Maintainability Symposium*, pages 392–397. IEEE, 2007.
- [30] Laurent Doyen and Olivier Gaudoin. Classes of imperfect repair models based on reduction of failure intensity or virtual age. *Reliability Engineering & System Safety*, 84(1):45–56, 2004.
- [31] David Applebaum. Lévy processes—from probability to finance and quantum groups. *Notices of the American Mathematical Society*, 51(11):1336–1347, 2004.
- [32] Zhi-Sheng Ye and Min Xie. Stochastic modelling and analysis of degradation for highly reliable products. *Applied Stochastic Models in Business and Industry*, 31(1):16–32, 2015.
- [33] Xiao-Sheng Si, Wenbin Wang, Chang-Hua Hu, and Dong-Hua Zhou. Remaining useful life estimation - A review on the statistical data driven approaches. *European Journal of Operational Research*, 213(1):1–14, 2011.
- [34] Khanh T.P. Nguyen, Mitra Fouladirad, and Antoine Grall. Model selection for degradation modeling and prognosis with health monitoring data. *Reliability Engineering & System Safety*, 169(August 2017):105–116, 2018.
- [35] Haitao Liao and Zhigang Tian. A framework for predicting the remaining useful life of a single unit under time-varying operating conditions. *IIE Transactions*, 45(9):964–980, 2013.
- [36] Qi Li, Zhanbao Gao, Diyin Tang, and Baoan Li. Remaining useful life estimation for deteriorating systems with time-varying operational conditions and condition-specific failure zones. *Chinese Journal of Aeronautics*, 29(3):662–674, 2016.
- [37] Julien Chevallier and Stéphane Goutte. On the estimation of regime-switching Lévy models. *Studies in Nonlinear Dynamics and Econometrics*, 21(1):3–29, 2017.

- [38] Nagi Z. Gebraeel, Mark A. Lawley, Rong Li, and Jennifer K. Ryan. Residual-life distributions from component degradation signals: A Bayesian approach. *IIE Transactions*, 37(6):543–557, 2005.
- [39] Linkan Bian and Nagi Gebraeel. Computing and updating the first-passage time distribution for randomly evolving degradation signals. *IIE Transactions*, 44(11):974–987, 2012.
- [40] Nagi Gebraeel and Jing Pan. Prognostic degradation models for computing and updating residual life distributions in a time-varying environment. *IEEE Transactions on Reliability*, 57(4):539–550, 2008.
- [41] Chao Ning and Fengqi You. A data-driven multistage adaptive robust optimization framework for planning and scheduling under uncertainty. *AIChE Journal*, 63(10):4343–4369, 2017.
- [42] Yannis A. Guzman, Logan R. Matthews, and Christodoulos A. Floudas. New a priori and a posteriori probabilistic bounds for robust counterpart optimization: I. Unknown probability distributions. *Computers & Chemical Engineering*, 84: 568–598, 2016.
- [43] Zukui Li, Ran Ding, and Christodoulos Floudas. A Comparative Theoretical and Computational Study on Robust Counterpart Optimization: I. Robust Linear Optimization and Robust Mixed Integer Linear Optimization. *Industrial & Engineering Chemistry Research*, 50(18):10567–10603, 2011.
- [44] Klaus; Pötzelberger and Liqun Wang. Boundary Crossing Probability for Brownian Motion and General Boundaries. *Journal of Applied Probability*, 34(1): 54–65, 1997.
- [45] Linkan Bian and Nagi Gebraeel. A stochastic methodology for prognostics under time-varying environmental future profiles. In *Proceedings of the 2011 Conference on Intelligent Data Understanding, CIDU 2011*, 2011.
- [46] Lothar Breuer. Occupation times for Markov-modulated Brownian motion. *Journal of Applied Probability*, 49(2):549–565, 2012.
- [47] Souleyman Ozekici. Optimal maintenance policies in random environments. *European Journal of Operational Research*, 82(2):283–294, 1995.

- [48] Lewis Paton, Matthias C M Troffaes, Nigel Boatman, Mohamud Hussein, and Andy Hart. Multinomial Logistic Regression on Markov Chains for Crop Rotation Modelling. *Information Processing and Management of Uncertainty in Knowledge-Based Systems*, pages 476–485, 2014.
- [49] Narayan Chanra Sinha, M. Ataharul Islam, and Kazi Saleh Ahamed. Logistic Regression Models for Higher Order Transition Probabilities of Markov Chain for Analyzing the Occurrences of Daily Rainfall Data. *Journal of Modern Applied Statistical Methods*, 10(1):337–348, 2011.
- [50] Fabian Pedregosa, Gaël Varoquaux, Alexandre Gramfort, Vincent Michel, Bertrand Thirion, Olivier Grisel, Mathieu Blondel, Peter Prettenhofer, Ron Weiss, Vincent Dubourg, Jake Vanderplas, Alexandre Passos, David Cournapeau, Matthieu Brucher, Matthieu Perrot, and Édouard Duchesnay. Scikit-learn: Machine Learning in Python. *Journal of Machine Learning Research*, 12: 2825–2830, 2012.
- [51] Cristian Bravo, Gaston L’Huillier, Jose Luis Lobato, and Richard Weber. Probability Estimation for Multiclass Problems Combining SVMs and Neural Networks. *Neural Network World*, 20(4):475–489, 2010.
- [52] Stephan Dreiseitl and Lucila Ohno-Machado. Logistic regression and artificial neural network classification models: A methodology review. *Journal of Biomedical Informatics*, 35(5-6):352–359, 2002.
- [53] Zhuangzhi Li and Zukui Li. Chance constrained planning and scheduling under uncertainty using robust optimization approximation. *IFAC-PapersOnLine*, 28(8):1156–1161, 2015.
- [54] Zhuangzhi Li and Zukui Li. Optimal robust optimization approximation for chance constrained optimization problem. *Computers and Chemical Engineering*, 74:89–99, 2015.
- [55] Donald R Jones, Matthias Schonlau, and William J Welch. Efficient Global Optimization of Expensive Black-Box Functions. *Journal of Global Optimization*, 13:455–492, 1998.
- [56] William E. Hart, Carl D. Laird, Jean-Paul Watson, David L. Woodruff, Gabriel A. Hackebeil, Bethany L. Nicholson, and John D. Sirola. *Pyomo – Optimization Modeling in Python*, volume 67. 2017.

- [57] William E. Hart, Jean Paul Watson, and David L. Woodruff. Pyomo: Modeling and solving mathematical programs in Python. *Mathematical Programming Computation*, 3(3):219–260, 2011.
- [58] Johannes Wiebe. STN with degradation. DOI: 10.5281/zenodo.1313718, 2018.
- [59] Miten Mistry, Andrea Callia D’Iddio, Michael Huth, and Ruth Misener. Satisfiability modulo theories for process systems engineering. *Computers and Chemical Engineering*, 113:98–114, 2018.
- [60] Andre A. Ciré, Elvin Çoban, and John N. Hooker. Logic-based Benders decomposition for planning and scheduling: A computational analysis. *Knowledge Engineering Review*, 31(5):440–451, 2016.
- [61] D. Letsios and R. Misener. Exact Lexicographic Scheduling and Approximate Rescheduling. *ArXiv e-prints*, arXiv:1805.03437, 2018.
- [62] Zukui Li, Qiuhua Tang, and Christodoulos A. Floudas. A Comparative Theoretical and Computational Study on Robust Counterpart Optimization: II. Probabilistic Guarantees on Constraint Satisfaction. *Industrial & Engineering Chemistry Research*, 51(19):6769–6788, 2012.
- [63] Linkan Bian and Nagi Gebraeel. Stochastic methodology for prognostics under continuously varying environmental profiles. *Statistical Analysis and Data Mining*, 6(3):260–270, 2013.
- [64] David Siegmund. Boundary Crossing Probabilities and Statistical Applications. *The Annals of Statistics*, 14(2):361–404, 1986.